Preserved structural property after amplification of alpha-synuclein aggregates
from brains of synucleinopathies

DOCTORAL DISSERTATION

A thesis submitted in partial fulfillment
of the requirements for the degree of
Doctor of Philosophy

By:
Saki Yoshinaga

Supervisor:
Dr. Nobuyuki Nukina

Co-Supervisor:
Dr. Tomoyuki Yamanaka
and
Dr. Haruko Miyazaki

Graduated School of Brain Science
Doshisha University
March 2020
Kyoto, Japan

Abstract

Many pathological proteins related to neurodegenerative diseases are misfolded, aggregating to form amyloid fibrils during pathogenesis. These pathological proteins can spread through neural network where the pathological proteins function as templates or "seeds" to misfold normal proteins. One pathological protein, alpha-synuclein (α-syn), accumulates in the brains of people with synucleinopathies, including Parkinson disease (PD), dementia with Lewy bodies (DLB), and multiple system atrophy (MSA). Recently, it has been suggested that structural properties of abnormal accumulated proteins determine the disease phenotype. However, the biochemical and structural characteristics of these accumulated proteins are still unclear due to an insufficient amount of fibrils for analysis. Previous studies in our group have reported on the sequence- and seed-structure-dependent polymorphic fibrils of α-syn and that their polymorphisms can be differentiated through their proteinase K-resistant fibril cores by mass spectrometry (MS) analysis.

This MS analysis was applied to investigate α-syn aggregates derived from MSA brains and DLB brains. To obtain a sufficient amount of α-syn aggregates for MS, recombinant α-syn fibrils were amplified by seeding reaction and protein misfolding cyclic amplification (PMCA) with seeds derived from diseased brains. MS analysis demonstrated that the characteristics of the proteinase K-resistant

cores of the aggregates pre and post amplification were preserved. Using the SDS-insoluble fraction of diseased brains as seeds, enough amplified α-syn fibrils were obtained to perform MS analysis of proteinase K-resistant cores. Furthermore, the structures of α-syn fibrils were observed using electron microscopy. Although no significant differences between amplified fibrils of MSA and DLB were observed by these approaches, the proteinase-resistant core analysis on the amplified abnormal protein fibrils with seeds derived from disease brains could be used for future studies of neurodegenerative disorders.

Acknowledgments

I thank to my considerate colleagues for their kind cooperation. Finally, I wish to extend my sincere gratitude to my family and friends for their understanding, support and encouragement throughout my study.

Table of Contents

List of Figures and Tables

Figures

Tables

Abbreviations:

PD: Parkinson disease

DLB: dementia with Lewy bodies

MSA: multiple system atrophy

α-syn: alpha-synuclein

WT: wild type

CBB: Coomassie Brilliant Blue

PMCA: protein misfolding cyclic amplification

ThT: thioflavin T

PFF: pre-formed fibril

PBS: phosphate-buffered saline

PFA: paraformaldehyde

FTA: filter trap assay

MS: mass spectrometry

MALDI-TOF MS: matrix assisted laser desorption ionization-time of flight mass spectrometry

EM: electron microscopy

Chapter 1. General Introduction

1.1. Misfolded protein aggregates in neurodegenerative disease

Neurodegenerative disorders have a common pathological feature: the aggregation and deposition of abnormal proteins [1]. The proteins most commonly implicated in the accumulation of cerebral misfolded aggregates in neurodegenerative diseases are amyloid-beta (Aβ), tau protein, alpha-synuclein (α-syn), and prion protein. These disease-associated proteins have no obvious similarities in respect of sequence, size, structure, expression level, and function [2]. Also, the depositions of these proteins exhibit different patterns and locations i.e. the progressive appearance and spread of lesions in human diseases [3]. Nevertheless, they all undergo misfolding from their native states to form intermolecular β-sheet-rich structures called amyloid in disease brains [4,5]. These amyloids are highly ordered fibrils, 100–200 Å in diameter, which consist of arrays of intermolecular β-sheets running parallel to the longitudinal axis of the fibrils. The structure is referred to as cross-β [6]. The method generally used to recognize amyloids is staining with specific dyes such as Thioflavin T (ThT) [7]. The detailed structure of amyloid is thought to differ greatly depending on the protein and the disease [5]. However, the biochemical and structural characteristics of these endogenous pathologically deposited proteins are still unclear.

1.2. Synucleinopathies

The α-syn protein is small, highly conserved, and is composed of 140-amino acids. Generally, α-syn is localized in the central nervous system, mainly in presynaptic nerve terminals. This protein plays important regulatory roles in areas including synaptic maintenance, mitochondrial homeostasis, proteasome function, dopamine metabolism, and chaperone activity [8].

α-syn was found to adopt a continuous α-helix from residues 9–89 on the surface of unilamellar vesicles as revealed via electron paramagnetic resonance (EPR) spectroscopy and nuclear magnetic resonance (NMR) spectroscopy [9, 10, 11]. Under certain conditions, α-syn spontaneously enters the amyloid state and self-assembles into amyloid oligomers and fibrils. Amyloid fibrils of α-syn were identified as a prominent component of the Lewy body, a molecular hallmark of PD [12, 13]. Over 90% of aggregated α-syn is phosphorylated at serine 129 (S129), while only about 4% of α-syn from normal brains are phosphorylated at this site [14, 15]. Therefore, antibodies recognizing α-syn phosphorylated at S129 are sensitive and can be specific tools for identifying the inclusions of synucleinopathies.

Synucleinopathies, including Parkinson disease (PD), dementia with Lewy bodies (DLB), and multiple system atrophy (MSA), are neurodegenerative diseases characterized by abnormal accumulation of insoluble α-syn aggregates in neuronal or glial cells in specific brain regions. These

pathological intracellular inclusions containing α-syn in selectively vulnerable neurons and glial cells are linked both to the onset and progression of clinical symptoms as well as the degeneration of affected brain regions (*Table 1*) [16]. Although the same protein α-syn accumulates in each synucleinopathy, the mechanisms and factors giving rise to each phenotype are not well understood.

Currently, it is unknown whether α-syn amyloids are the cause or a consequence of synucleinopathy. However, the neuroinflammation from lipopolysaccharide injections in control mice led to a significant loss of tyrosine hydroxylase-positive neurons in the substantia nigra with the accumulation of insoluble aggregated α-syn as cytoplasmic inclusions, as compared to α-syn knockout mice [17]. Thus, it is likely that α-syn amyloids cause synucleinopathy.
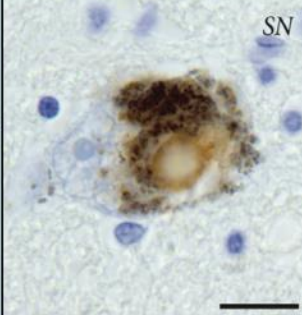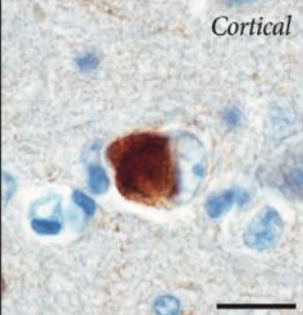
Main types of α-synucleinopathy	Parkinson's disease (PD)	Dementia with Lewy bodies (DLB)	Multiple system atrophy (MSA)
Location of accumulation	SNpc of midbrain	Spread diffusely from cerebral cortex to brain	White matter of cerebellum and basal ganglion
Cell	neuron		oligodendroglia
The accumulation and aggregation of α-synuclein	NCIs — SN	NCIs — Cortical	GCIs — Pons

Table 1. The differences between the three main synucleinopathies, Parkinson disease (PD), dementia with Lewy bodies (DLB) and multiple system atrophy (MSA).

PD and DLB have intraneuronal α-syn inclusions known as Lewy bodies, and MSA has glial cytoplasmic inclusions (GCIs). Photomicrographs show α-syn immunoreactive structures counterstained with cresyl violet. NCIs: indicates neuronal cytoplasmic inclusions, SN: substantia nigra, scale bar = 25 µm. The images were modified from [16].

1.3. Conformational strains of misfolded protein

Protein aggregation is an important and generic aspect of protein energy landscapes [18]. In protein energy landscapes, a polypeptide chain has been proposed to exist not only in native conformation but also in alternative structures such as amyloid structures. Compared to the natively folded structure, amyloid fibrils have considerably higher stability and relatively lower energy state.

The energy landscapes model highlights many different conformational states available to a protein (Figure 1) [19].

The remarkable ability of a small number of proteins such as α-syn and tau give rise to multiple diseases called synucleinopathies and tauopathies, each with unique symptoms, progressions, and neuropathologies. These diseases are thought to occur as a result of the protein misfolding into a distinct conformation [20].

Identification of the missense mutations in the α-syn gene in some pedigrees of familial PD is strongly implicated in the pathogenesis of PD and other synucleinopathies [21]. Recent studies in our group have indicated that disease-related mutants of α-syn formed aggregates *in vitro*, exhibiting distinct sequence and structure-dependent biochemical and morphological properties compared to normal α-syn [22, 23]. The disease phenotypes are different among patients exhibiting these mutations, suggesting that the difference of the structures of α-syn aggregates could be responsible for the various pathologies and phenotypes.

As with viral strains, pathogenic proteins related to diseases with different phenotypes but with the same protein accumulation, are also differentiated as strains. To identify a unique pathogenic structure for distinct phenotypes, Sanders *et al*. [24] developed a cell system to isolate tau strains from patients with 5 different tauopathies and showed that each disease is associated with different sets of

strains. They transduced lysates from each clone into naive tau RD-YFP cells, and monoclonal

inclusion-containing cells were isolated and amplified. Their findings indicated that an individual

protein may have variations of misfolded structures. Also, using recombinant human α-syn, it has been

proposed that distinct α-syn strains display differential seeding capacities, inducing strain-specific

pathologies and neurotoxic phenotypes. Concretely, ribbon-type fibrils led to Lewy pathology when

they were injected into the rat substantia nigra [25]. Using cryo-electron microscopy, recent studies

have shown that full-length recombinant human α-syn has the structures of two predominant species:

a rod and a twister [26]. The results of these studies suggest the possibility that structural properties of

abnormal accumulated proteins could determine the disease phenotype.
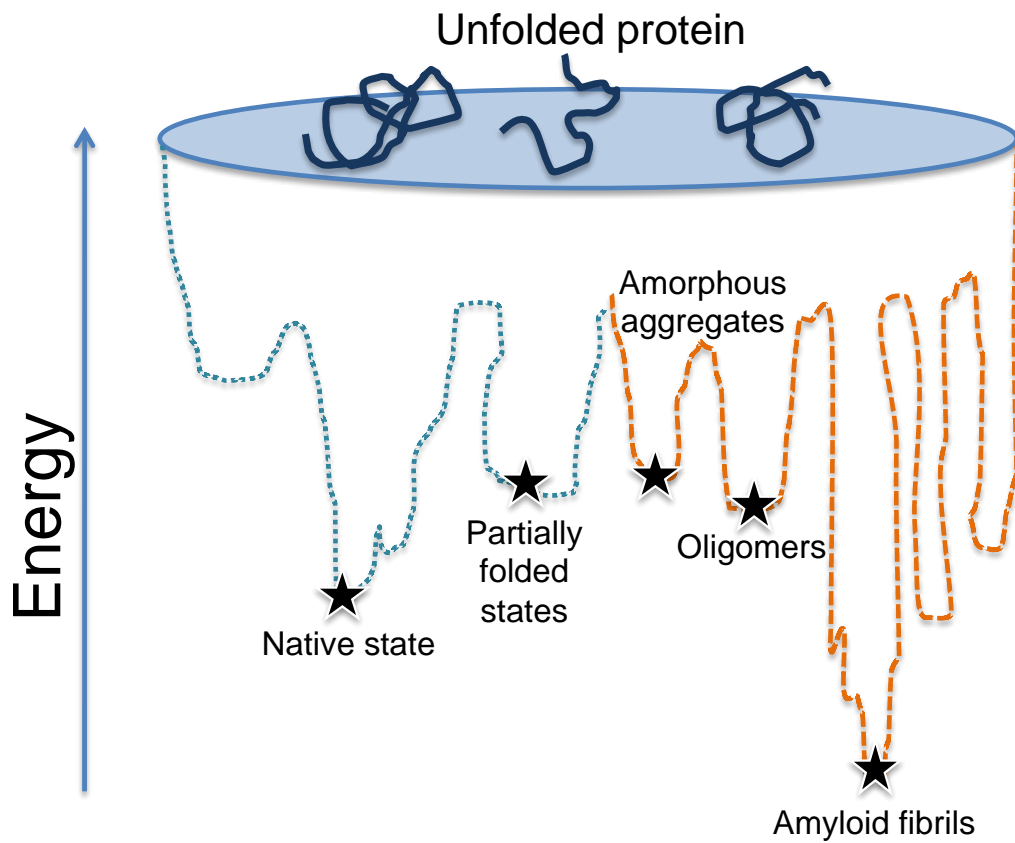
Figure 1. A schematic model of folding and misfolding energy landscapes.

The blue and orange dotted lines indicate the folding and misfolding landscapes respectively. The image was modified from [18].

1.4. Prion protein and other proteins of neurodegenerative diseases

Misfolded aggregates of amyloid fibrils are associated with neurodegenerative diseases. Among these, prion diseases are unique in that the pathology can cause host-to-host transmission via infection [27]. Prions are infectious proteins that may transmit biological information by propagating misfolded proteins and aggregations [28]. According to several studies, the molecular mechanism of prion conversion bears a strong resemblance to the amyloid formation process, indicating that misfolded aggregates possess an inherent ability to be transmitted [29]. At the molecular level, the template-induced conversion of natively folded proteins by misfolded proteins results in autocatalytic growth of protein aggregates [30]. At the cellular level, the pathology spreads from cell to cell via transfer of misfolded protein aggregates between adjacent cells, resulting in regional spreading of the dysfunctions [31]. At the organ level, the progressive transmission and spread of the pathology occur between remote areas of the brain, either through cell-to-cell contact or via biological fluids such as the interstitial fluid, the cerebrospinal fluid, or the blood [32, 33]. However, unlike prion diseases, in which host-to-host transmission occurs like infection, it appears that in other protein misfolding disorders, these misfolded proteins spread only at the molecular, cellular, and tissue levels, but not at the individual level [29].

1.5. Seeding reaction and protein misfolding cyclic amplification (PMCA)

At the molecular level, aggregated proteins function as templates or "seeds" to facilitate misfolding of substrate proteins during fibrillization. This reaction is known as the amyloid seeding reaction. From a biophysical perspective, the process of protein misfolding and aggregation involves the structure of the protein being rearranged into a series of rich β-sheets (Figure 2) [34]. Protein Misfolding Cyclic Amplification (PMCA), a practical application of the seeding reaction originally developed for prions, enables efficient amplification of the amyloid seeds by repeating cycles of ultrasonic fragmentation of seeds and fibrillization *in vitro*. Amplification is based on multiple cycles of incubation of misfolded proteins in the presence of an excess of natively folded proteins, followed by sonication. During incubation, the size of the oligomeric misfolded proteins increases due to the structural change of native proteins into the aggregated misfolded proteins. With aggregate disruption during sonication, an expanded population of converting units produced (Figure 3) [35]. Although PMCA promotes the rate of self-aggregation, it helped in detecting pathological proteins at extremely low concentrations.

For the past several years, PMCA was used only for amplification of misfolded prions as recombinant prions may not cause self-aggregation. However, a recent study has shown that misfolded

tau proteins may also be amplified with PMCA [36], suggesting the possibility that PMCA could

amplify misfolded α-syn [37].

As of now, few studies have been performed to test the accuracy of PMCA as a tool for

diagnosing synucleinopathies. While the ideal detectable concentration of misfolded α-syn has been

simulated, these previous studies did not show high signals of misfolded α-syn. Accordingly, to verify

the hypothesis that misfolded α-syn could be detected from concentrations as low as 2 pg using PMCA

as a diagnostic tool, various concentrations of misfolded α-syn were seeded in recombinant human α-

syn.
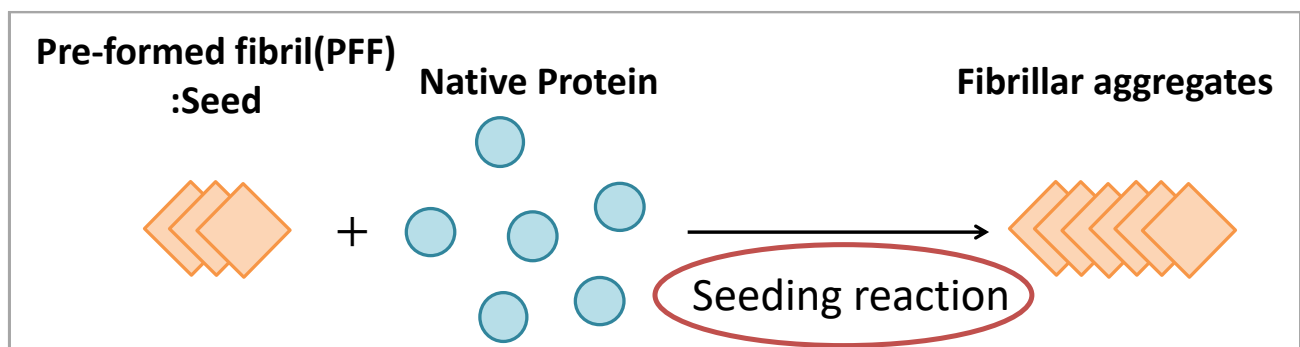
Figure 2. The mechanism of seeding reaction

The formation of fibrillar aggregates (orange squares) is accelerated greatly by recruiting native proteins (blue circles) into the aggregates (seeds; orange squares).
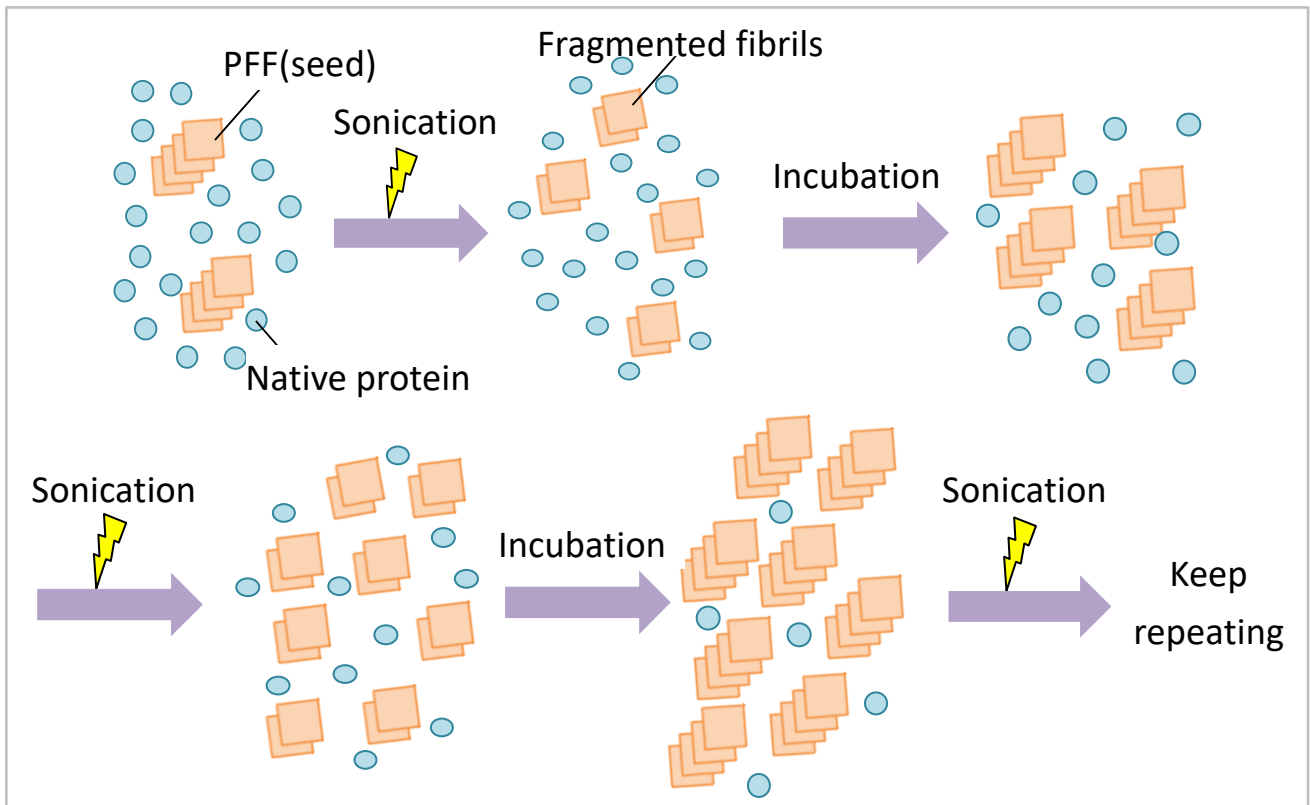
Figure 3. Diagrammatic representation of the PMCA procedure.

The blue circles denote folded proteins, and the orange squares denote misfolded proteins. The PMCA procedure was repeated until self-aggregation occurred.

1.6. Homogenates isolated from human brain

The homogenates of the brains of patients with neurodegenerative diseases are rich in different kinds of amyloid fibrils depending on the disease [4]. The insoluble protein fractions from disease brains contain not only abnormal fibrils specific to the disease but also non-specific insoluble proteins such as lipofuscin, which makes it difficult to obtain pure amyloid fractions. The fibrils in the

brain also have post-translational modifications, including ubiquitination. All in all, these hinder the

study of structural and biochemical properties of α-syn aggregates. In the current study, α-syn fibrils

were amplified by seeding reaction and PMCA using the insoluble protein fractions of α-

synucleinopathies, and their properties were investigated.

Chapter 2. Materials and Methods

Purification of recombinant α-syn: Purification of His-tagged human and mouse α-syn has been

described previously [38]. *E. coli* BL21 (DE3) were transformed using the expression vector pET-15b,

encoding either human or mouse α-syn, and were then cultured overnight in 25 ml LB medium

including 50 µg/ml ampicillin (LB amp$^+$) and transferred to 250 ml LB amp$^+$ until the measured optical

density (OD = 600 nm) reached 0.6 using BioSpectrometer® (Eppendorf). 1 mM Isopropyl-β-D-

thiogalactopyranoside was added, and the mixture was incubated for 6 h at 37 °C and then centrifuged

at 3,000xg for 30 min at 4 °C. Phosphate-buffered saline (PBS) with 2% TritonX-100 was added to

the resulting pellet, and centrifugation at 20,000xg for 30 min at 4 °C was performed. Ni-sepharose

beads (1 ml, GE Healthcare) were added to the supernatant obtained to capture the α-syn and incubated

rotating for 1 h, at 4 °C. The beads were washed using buffer A (50 mM Tris-HCl pH 8.0, 100 mM

NaCl) containing 10 mM imidazole, and the α-syn was then eluted using buffer A including 250 mM

imidazole. The eluted samples were concentrated via centrifugation at 3000xg for 15 min with

Vivaspin Turbo tubes (15 K MW) (50 ml, Sartorius). The collected α-syn was treated with thrombin

agarose (Sigma) and rotated for 20 h at 20 °C to cleave the N-terminal His-tag. The α-syn with the

His-tag removed was obtained via filtration using a 0.22 µm filter. The concentration of α-syn protein

was ascertained by its absorption at 280 nm with the BioSpectrometer® (Eppendorf). The monomeric

forms of α-syn adjusted to 100 μm were stored at −80 °C. Before these α-syn monomers were used, thawed samples were ultracentrifuged at 153,700xg for 1 h at 4 °C to avoid the effects of self-aggregation.

Preparation of seeds from recombinant α-syn: The method for the formation of seeds from recombinant α-syn has been described previously [22]. Purified α-syn monomers (100 μM, 150 µl) were agitated in buffer A with plastic beads (Sanplatec) using DWMax M•BR-034 (TAITEC) at 1,000 r/min for 7 d at 37 °C. Aggregates were pelleted via ultracentrifugation at 153,700xg for 1 h at 4 °C, resuspended in buffer A (150 µl) and then ultracentrifuged once more. These aggregates were resuspended in buffer A (150 µl) and sonicated using Bioruptor (Biorad). They were used in experiments as "pre-formed fibrils (PFFs)."

Seeding reaction and PMCA: For a seeding reaction, 5 µl (5%vol) of either PFF or P4 fraction from brain homogenate was added to the monomeric form of α-syn (20 μM) in 95 µl of buffer A. Seeding efficiencies were evaluated every 1 min by Thioflavin-T fluorescence (25 μM) using Spectra Max (Molecular Devices). The species (either mouse or human) for the monomeric form of α-syn corresponded to that for the seed. Once aggregates were formed, the solution was ultracentrifuged at

153,700xg for 1 h at 4 °C. After 40 h and 100 h seeding reactions for mouse α-syn and human α-syn, respectively, the aggregations obtained were resuspended in 25 μl buffer A and sonicated using Bioruptor. For PMCA, 5 μl of the resuspended solution was added to 95 μl of the monomeric forms of α-syn (20 μM). ELESTEIN 070-CPR (ELEKON SCIENCE CO.) was used for PMCA, with sonication set for 25 sec and incubation set for 30 min at 37 °C. The reaction cycles were set 80 times for mouse α-syn and 200 times for human α-syn. Kinetics of aggregation of α-syn were assessed by Thioflavin-T fluorescence (25 μM) using Spectra Max both before and after PMCA reaction. After PMCA, the solution was ultracentrifuged at 153,700xg for 1 h at 4 °C, and the obtained aggregates were resuspended in 25 μl of buffer A and sonicated.　summarizes the procedure.

Mass spectrometry analysis of the proteinase K-resistant core: The method has been described previously [19]. α-syn aggregates were treated with proteinase K (4 μg/ml) for 120 min at 37 °C for analysis of the amyloid core. Proteinase-resistant amyloid fibrils were pelleted via ultracentrifugation at 153,700xg for 30 min. The pellets were dissolved in 3.33 mM Tris-HCl, 2 M Guanidine hydrochloride, and 0.033% Trifluoroacetic acid. The dissociated amyloid fibril peptides were desalted using self-made C18 (3 M Empore solid phase extraction disk) Stage Tip and analyzed using MALDI-TOF MS (autoflex speed TOF/TOF, Bruker Daltonics).

Preparation of mouse brain: 8-week-old male C57BL/6J mice were obtained from CLEA Japan, Inc. The mice were housed under a 12-h light/12-h dark cycle with access to food and water and at a maximum of five per cage. The breeding and housing of the mice were done according to the guidelines for Animal Care of Doshisha University and were approved by the Doshisha University Animal Care and Use Committee. The method of mouse brain injection has been described previously. For intracerebral injection, α-syn PFFs were sonicated until an isocratic solution was obtained using Bioruptor (Biorad). Mice were anesthetized via peritoneal injection of pentobarbital, and 5 μg/ μl of recombinant mouse α-syn PFFs were injected unilaterally into the right striatum (A-P: 0.3 mm; M-L + 2 mm; D-V: − 2.5 mm, from bregma) using a 10 μl Hamilton syringe at a rate of 0.5 μl per min. instead of PFFs, PBS was injected into control mice. After three months, the injected mice were sacrificed by cervical dislocation. The brains were removed from the injected mice and stored in separate brain hemispheres.

Preparation of brain homogenates: All mouse samples included tissue from the injection-side brain for mouse α-syn PFF injected mice and PBS injected mice. Human brain tissue samples were obtained

from Brain Bank in Japan. The samples included tissues from the insular gyrus of MSA patients, DLB

patients, and controls (Table 2 lists the information about the brains).

Case	Age	Sex	LB score
MSA-1	76	Male	0
MSA-2	71	Female	0
MSA-3	77	Male	0
MSA-4	59	Male	0
MSA-5	68	Male	0
DLB-1	77	Male	5
DLB-2	74	Female	5
DLB-3	74	Male	5
DLB-4	76	Male	4
DLB-5	72	Male	4
Control-1	70	Male	0
Control-2	70	Male	0
Control-3	70	Female	0
Control-4	75	Female	0
Control-5	69	Male	0

Table 2. Information about the human brains used in this study.

Note. Human brain tissue samples were obtained from Brain Bank in Japan. Human samples were
from the insular gyrus of MSA patients, DLB patients, and controls. The brains were assessed

pathologically for their LB scores calculated from sections and stained with H&E and anti-ubiquitin immunohistochemistry, as recommended by the consensus guidelines for DLB [31].

The pathology of the insular cortices in DLB at the stage of dementia has been described in previous study [29]. Moreover, previous studies have reported that the GCIs were discovered with the insular cortices. Following the protocols reported previously [40, 41], mouse and human brains in nine volumes (v/w) of ice-cold buffer B [10 mM Tris-HCl pH 7.6, 0.8 M NaCl, 10% sucrose, 0.1% Triton X-100, 50 mM NaF, 1 mM Na_3Vo_4, cOmplete^{TM} (Sigma-Aldrich, 1 tablet/ 50 ml)] were homogenized on ice 10 times each via extrusion through 18 and 21 gauge needles. The homogenates were centrifuged at 1000xg for 5 min at 4 °C. The supernatants (S1) were collected, and the pellets were rehomogenized for 10 times in 9 volumes (v/w) of buffer B through a 21-gauge needle. Rehomogenized samples (S2) were centrifuged at 1000xg for 5 min at 4 °C and combined with S1 (S1+S2). S1+S2 was incubated with 1% Sarkosyl and 0.2% dithiothreitol at room temperature for 2.5 h, rotating. The samples were ultracentrifuged at 180,000xg for 3 h at 4 °C, and the pellets were resuspended in buffer A and ultracentrifuged again. The resultant pellet was designated as P3. P3 was suspended with buffer A including 1% SDS and 1% mercaptoethanol, sonicated, and heated for 5 min at 100 °C. After heat treatment, the samples were ultracentrifuged at 180,000xg for 3 h at 20°C and

washed with buffer A. The pellet (P4) was then resuspended in one volume (v/weight of the original

brain) of buffer A, sonicated, and stored at -80 °C. Figure 8B summarizes the procedure.

Antibody: The antibodies used in this study were anti-phospho-alpha-synuclein antibody (anti-p-syn

#64, Wako) and anti-alpha-synuclein antibody [MJFR1] (ab209420, Abcam).

Immunostaining: SDS-insoluble pellets (P4) of human brain tissue samples were smeared on a

microscope slide and dried overnight. The smears were fixed with 4% paraformaldehyde (PFA)/ PBS

for 20 min and blocked for 30 min with TBS-T (20 mM Tris–HCl, pH 8.0, 150 mM NaCl, 0.05%

Tween-20) containing 0.1% TritonX-20 and 2.5% goat serum. The sections were then incubated

overnight at 4 °C with the primary antibody (anti-p-syn #64, Wako) diluted with TBS-T containing

0.1% bovine serum albumin (BSA). They were incubated with the biotinylated secondary antibody,

followed by ABC reagent (Vector), and then detected with diaminobenzidine (DAB) staining.

SDS-polyacrylamide gel electrophoresis and Western Blotting: For SDS-polyacrylamide gel

electrophoresis (SDS-PAGE), 5 µl of samples were mixed with 5 µl of 2xSDS-PAGE sample buffer

(100 mM Tris-HCl, pH 6.8, 4% SDS, 2% 2-Mercaptoethanol, 20% Glycerol, and 0.01% bromophenol

blue). Before electrophoresis, the samples were heated for 5 min at 100 °C. 12% SDS containing

polyacrylamide gels (6.25% stacking gel) were used for electrophoresis at 20 mA for 75 min at room

temperature with running buffer (100 mM Tris, 100 mM glycine, and 0.1% SDS). The gels were

stained with Coomassie Brilliant Blue (CBB). For Western blotting (WB), The proteins were

transferred from the gel to the transfer membrane, Immobilon-P (Merck). The membrane was fixed

with 4% PFA and 0.01% glutaraldehyde/ PBS for 20 min [42] and blocked with 5% skim milk in TBS-

T. The membrane was incubated overnight at 4 °C with a primary antibody (anti-p-syn #64, Wako)

diluted with TBS-T containing 3% goat serum. The proteins were then reacted with horseradish

peroxidase (HRP)-secondary antibody in the same buffer. Chemiluminescent signals were obtained

using Immobilon Forte Western HRP Substrate (Merck) and quantified with ImageQuant LAS-4000

(GE).

Filter trap assay: A filter trap assay (FTA) was conducted to detect the amount of insoluble high

molecular weight α-syn aggregates using a Hybri-Dot Vacuum manifold (No.1050MM, BRL) and a

cellulose acetate membrane filter with a pore size of 0.2 μm (Advantec), as described previously [43].

5 μl of fractionated brain samples were mixed with in 100 μl of TBS-T and applied to the apparatus.

Soluble proteins were removed via vacuum suction, and the SDS-resistant aggregates remained

trapped. Wells were washed three times with PBS, and suction was maintained for 20 min. The

membranes were then blocked with 5% skim milk, and immunostaining and detection were carried

out for WB.

Electron microscopy: Morphological observations of α-syn fibrils were made using an electron

microscope H-7000 (Hitachi) at an accelerating voltage of 100 kV. The samples were adsorbed on

400-mesh grids coated by a glow-charged supporting amorphous carbon film and negatively stained

with 2% uranyl acetate.

Chapter 3. Results

3.1 The detection of seed fibrils amplified by protein misfolding cyclic amplification (PMCA) using recombinant human α-syn

The efficiency of PMCA with misfolded recombinant human α-syn was examined. ThT fluorescence intensity was measured from seeding using misfolded recombinant human α-syn at a final concentration ranging from 0.5 nM to 50 fM in the presence of buffer A (Figure 4). Amyloids form much more rapidly when misfolded recombinant human α-syn was added to the reaction. The ThT fluorescence intensity of PMCA began to increase at 24 h, whereas that of unseeded reactions showed no increase even at 70 h.
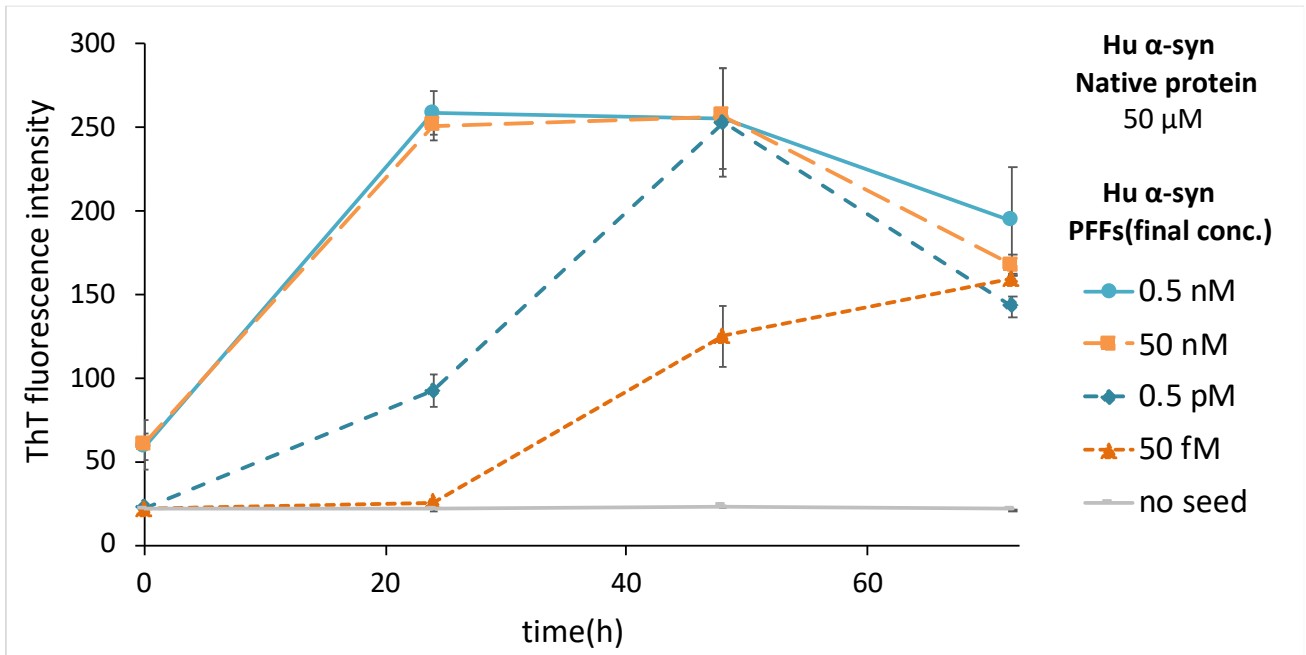
Figure 4. PMCA of misfolded recombinant human α-syn is concentration-dependent.

PMCA was conducted in the presence of buffer A with a distinct concentration of recombinant human α-syn seeds. The lowest concentration of seeds was 50 fM, and the highest was 0.5 nM. The concentration of the native recombinant human α-syn substrates was 50 µM.

3.2 Amplification of recombinant α-syn

Spontaneously aggregated recombinant mouse and human α-syn were obtained and used as seeds. Amplified aggregates were obtained after seeding reaction (A1) and PMCA (A2) with recombinant α-syn (Figure 5). In the seeding reaction, the concentration of recombinant α-syn pre-formed fibrils (PFFs) was 100 µM, and the substrate concentration was 20 µM. The seed and the

substrate were reacted in a ratio of 1 to 19 (Table 3). Amyloid fibrils were formed readily, as measured

via ThT fluorescence intensity.

PFFs or P4 solution (seeds)

5 % vol.

monomer
(20 µM)

95 % vol.

Seeding reaction
153,700 × g, 4 ℃, 1h

+ resuspend buffer A

A1 solution

5 % vol.

monomer
(20 µM)

95 % vol.

Protein Misfolding
Cyclic Amplification (PMCA)
153,700 × g, 4 ℃, 1h

+ resuspend buffer A

A2 solution

Figure 5. Schematic description of the procedure of seeding reaction and PMCA using recombinant α-syn aggregates.

A1 solution: amplified aggregates after seeding reaction; A2: amplified aggregates after PMCA.

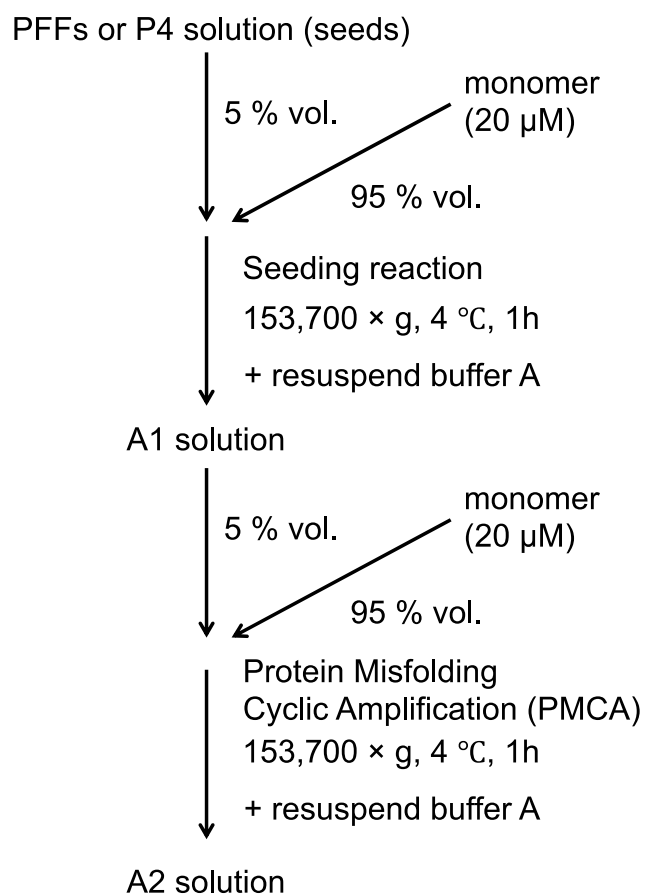|		Seed	Substrate
1	self aggregation	Mouse PFF	
2	seeding reaction	Mouse PFF	Mouse α-syn
3		Buffer	Mouse α-syn
4	PMCA	2 after seeding reaction	Mouse α-syn
5		3 after seeding reaction	Mouse α-syn
6		Buffer	Mouse α-syn
7	self aggregation	Human PFF	
8	seeding reaction	Human PFF	Human α-syn
9		Buffer	Human α-syn
10	PMCA	8 after seeding reaction	Human α-syn
11		9 after seeding reaction	Human α-syn
12		Buffer	Human α-syn

Table 3. A list of seeds and substrates for seeding reaction and PMCA.

Note: The list numbers in this table are used in Figure 6, Figure 7, Figure 11 and Figure 16.

When PFFs was added to the reaction, amyloid formation accelerated considerably. For the recombinant mouse α-syn, the reaction cycles of PMCA after the seeding reaction were set for 80 times, sonication for 25 sec, and incubation for 30 min at 37 °C. There was a large increase in the ThT fluorescence signal in PMCA seeded by mouse PFFs compared to that of the control (Figure 6A). On the other hand, for the recombinant human α-syn, the reaction cycles of PMCA were set for 100 times, sonication set for 25 sec, and incubation set for 30 min at 37 °C after the seeding reaction. There was also a great increase in the ThT fluorescence signal for PMCA seeded by human PFF compared to the control (Figure 7A). SDS-PAGE was conducted using those amplified products. As shown in Figure

6B and Figure 7B, mouse and human recombinant α-syn fibrils respectively were amplified

sufficiently by seeding reaction and PMCA using recombinant PFFs. Misfolded α-syn were amplified

with the synergistic method of both seeding reaction and PMCA.
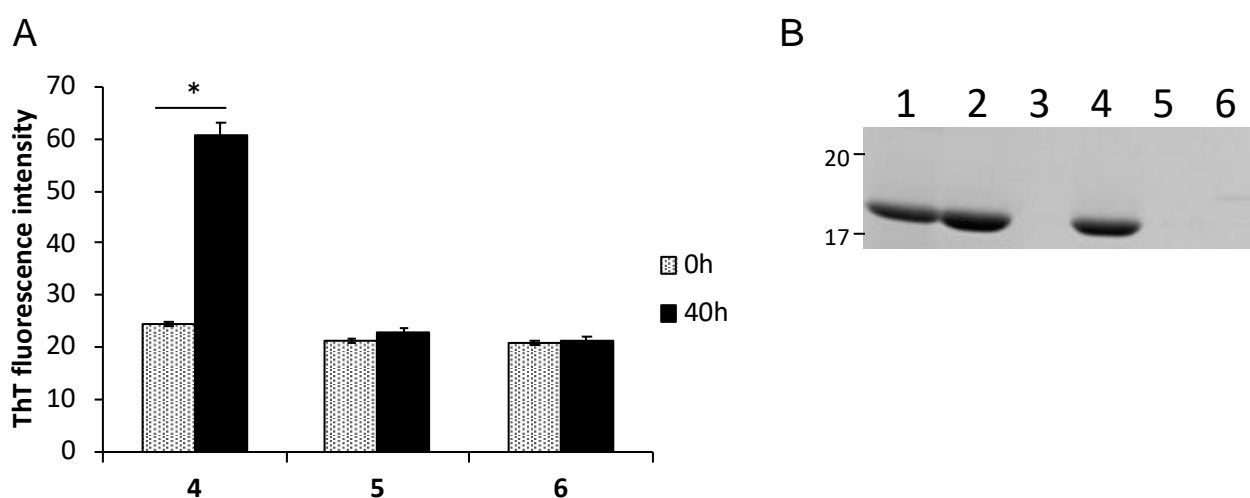

Figure 6. Recombinant mouse PFFs enable native recombinant mouse α-syn to form amyloid aggregates.

(A) ThT fluorescence intensity of PMCA at 0 h and 40 h (4: Mouse PFF after seeding reaction; 5: Buffer after seeding reaction; 6: Buffer). $^*p < 0.01$ (B) PFF (1), aggregations after seeding reaction (2), and PMCA (4) were detected by SDS-PAGE. The gels were stained with CBB.

A

B
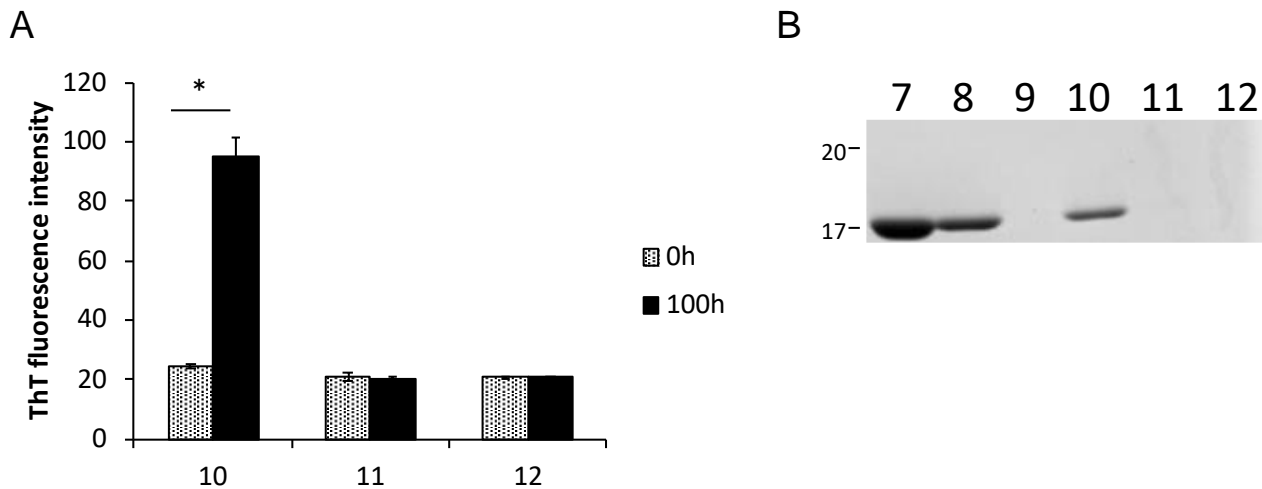
Figure 7. Recombinant human PFFs enable native recombinant human α-syn to form amyloid aggregates.

(A) ThT fluorescence intensity of PMCA at 0 h and 100 h (10: Human PFF after seeding reaction; 11: Buffer after seeding reaction; 12: Buffer). *p < 0.01(B) PFF (7), aggregations after seeding reaction (8), and PMCA (10) were detected by SDS-PAGE. The gels were stained with CBB.

3.3. The preparation of seed-enriched fraction from the B6J mouse brains

Either aggregated α-syn (5 μg/μl) or PBS were injected into B6J mice. 90 d after injection (Figure 8A), the mouse brains were fractionated (Figure 8B). The WB of sarkosyl-insoluble pellets (P3) from B6J mouse brains of 90 d after the aggregated α-syn injection were stained with anti-phosphorylated-α-syn antibodies. The bands of α-syn (monomer, dimer, and aggregation) in the P3 fraction of aggregated-α-syn-injected mouse brains were detected (Figure 9). A higher molecular weight polypeptide around 30 kDa may correspond to either ubiquitinated α-syn species [45] or non-

specific binding due to the mouse derived antibody. Amyloid seeding reactions using the P3 fractions and SDS-insoluble pellets (P4) from B6J mouse brains 90 days after the injection with aggregated α-syn as seeds were monitored via ThT assay (Figure 10). The seeding reaction of the P4 fractions was more effective than that of the P3 fractions. This indicates that the P4 fractions were more seed-enriched than the P3 fractions. Amyloid seeding reactions of the P4 fractions from additional B6J mouse brains 90 days after the injection with aggregated α-syn were monitored via ThT assay (Figure 11A). After the seeding reaction and PMCA, a large increase in the ThT fluorescence signals was observed in the samples seeded by the P4 fractions of the mouse brain injected with mouse α-syn, compared to the control (Figure 11B). The P4 fractions of the mouse brain injected by mouse α-syn seeds did not display α-syn bands with WB stained by an anti-α-syn antibody [ab209420 (Abcam)]. Aggregates of mouse α-syn amplified by seeding reaction and PMCA were examined with SDS-PAGE stained by CBB. Although the amplified fibrils of all samples of mouse brain injected with mouse α-syn seeds showed no α-syn bands in CBB staining with only using the seeding reactions (A1), after PMCA (A2), α-syn bands could be detected (Figure 11C). Sufficient amounts of aggregates for proteinase digestion and MS analysis were therefore obtained.
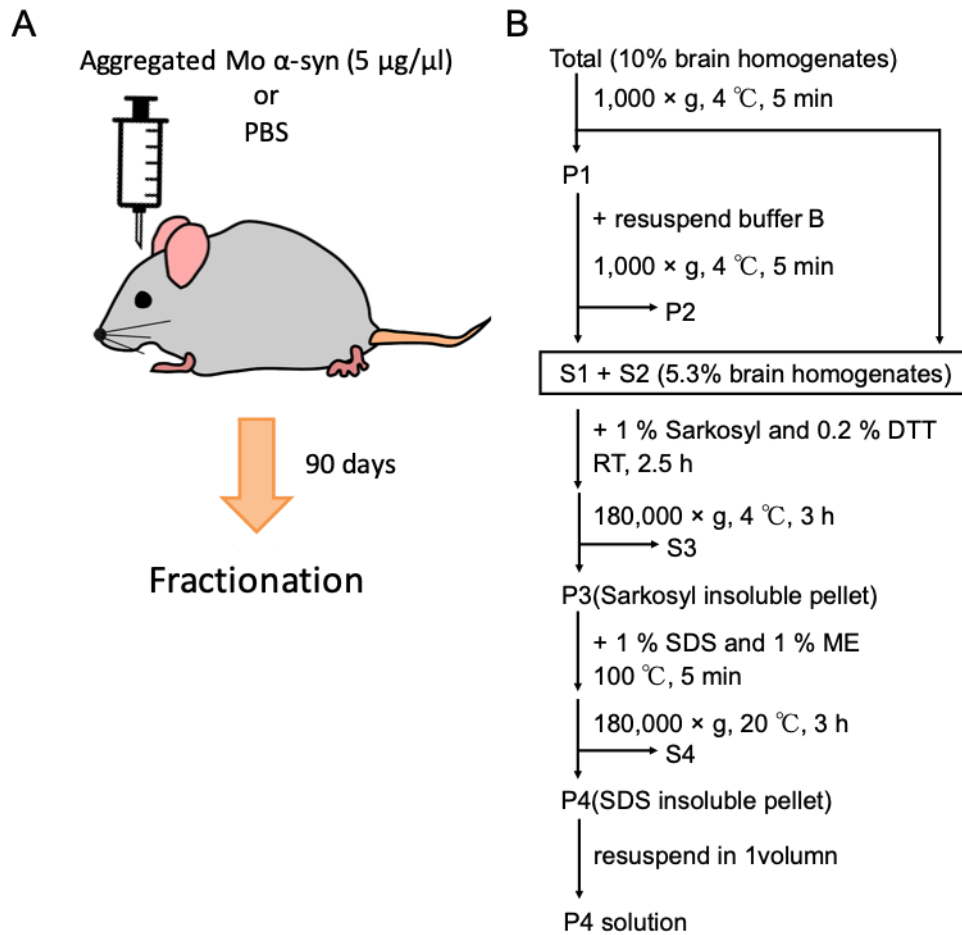
Figure 8. Preparation of seed-enriched fractions from the B6J mouse brains.

(A) Schematic illustration of the injection with either aggregated α-syn (5 μg/μl) or PBS into B6J mice. After 90 d, the mouse brains were fractionated. (B) The scheme was used in from Figure 9 to Figure 17.

1	Total
2	S1
3	P1
4	Total2
5	S2
6	P2
7	Total3(S1 + S2)
8	S3
9	P3
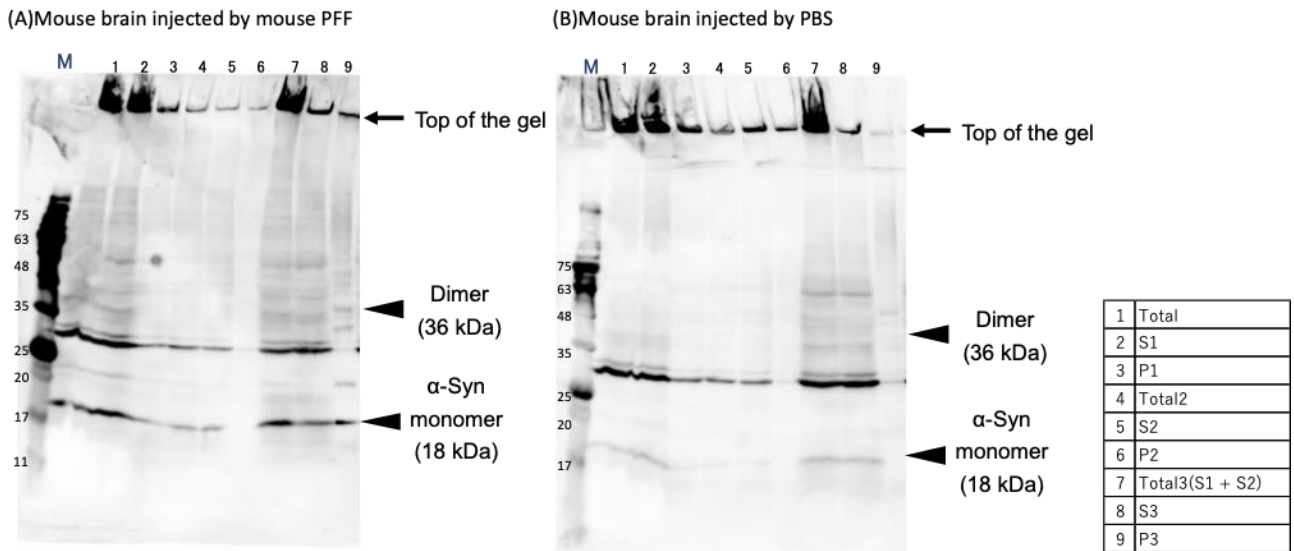
Figure 9. Cerebral misfolded α-syn aggregates are detected in the sarkosyl-insoluble fraction of the aggregated α-syn-injected mouse brain.

(A) WB of the sarkosyl-insoluble fractions (P3) derived from aggregated α-syn-injected mouse brain stained by anti-p-syn antibody (Wako). Bands of α-syn (monomer: 18kD; dimer: 36kD; aggregation: high molecular) in lane 9 (sarkosyl-insoluble fraction) were detected. (B) WB of PBS-injected mouse brain fractionations by anti-p-syn antibody (Wako). No bands of α-syn observed in (A) were detected in lane 9.
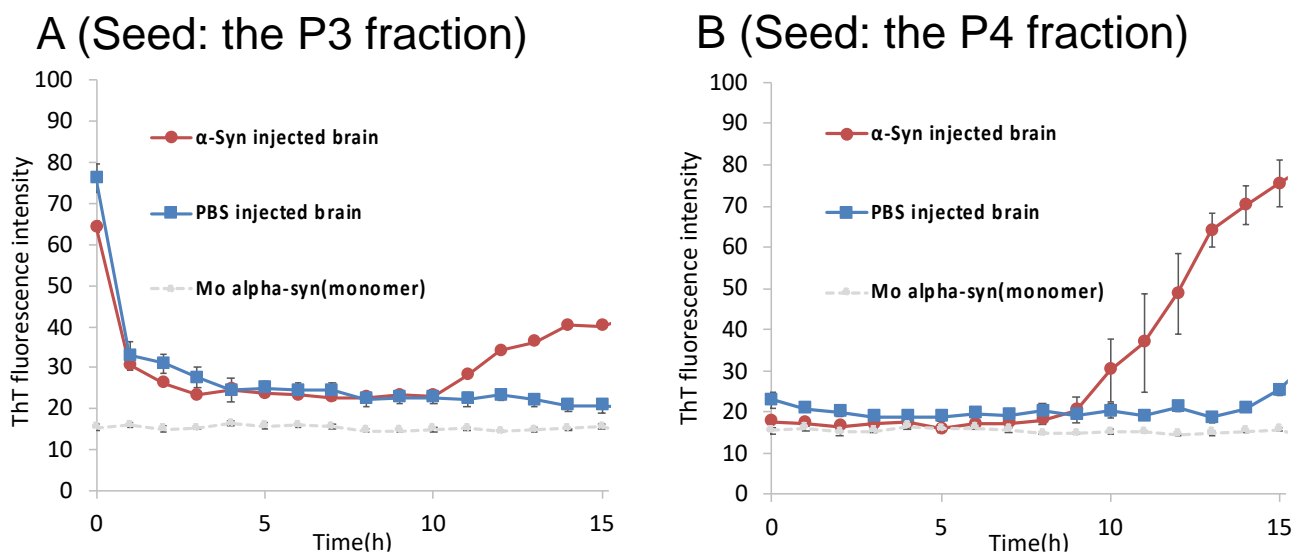
Figure 10. Seeding reactions with the seed derived from the P3 fraction and the seed of the P4 fraction in mouse brains.

(A) The kinetics of recombinant mouse α-syn amyloid formation monitored by ThT fluorescence using the P3 fraction as seeds. Recombinant mouse α-syn was incubated in solution A1 with 5% of the P3 fraction in α-syn injected brain (circle). As control, the P3 fraction derived from PBS-injected brain (square) and only monomer (dot) were used for the reactions. (B) The kinetics of recombinant mouse α-syn amyloid formation monitored by ThT fluorescence using the P4 fraction as seeds. Recombinant mouse α-syn was incubated in solution A1 with 5% of the P4 fraction in α-syn-injected brain (circle). As control, the P4 fraction derived from PBS-injected brain (square) and only monomer (dot) were used for the reactions.

Figure 11. The P4 fractions of mouse α-syn-injected mouse brains induce formation of amyloid aggregates from native recombinant mouse α-syn.

Three mice (a-c) were injected with mouse α-syn PFF. Their P4 fractions were used for seeding reaction; As control, the P4 fractions of PBS injected mouse brains (d, e) were used for seeding reaction. (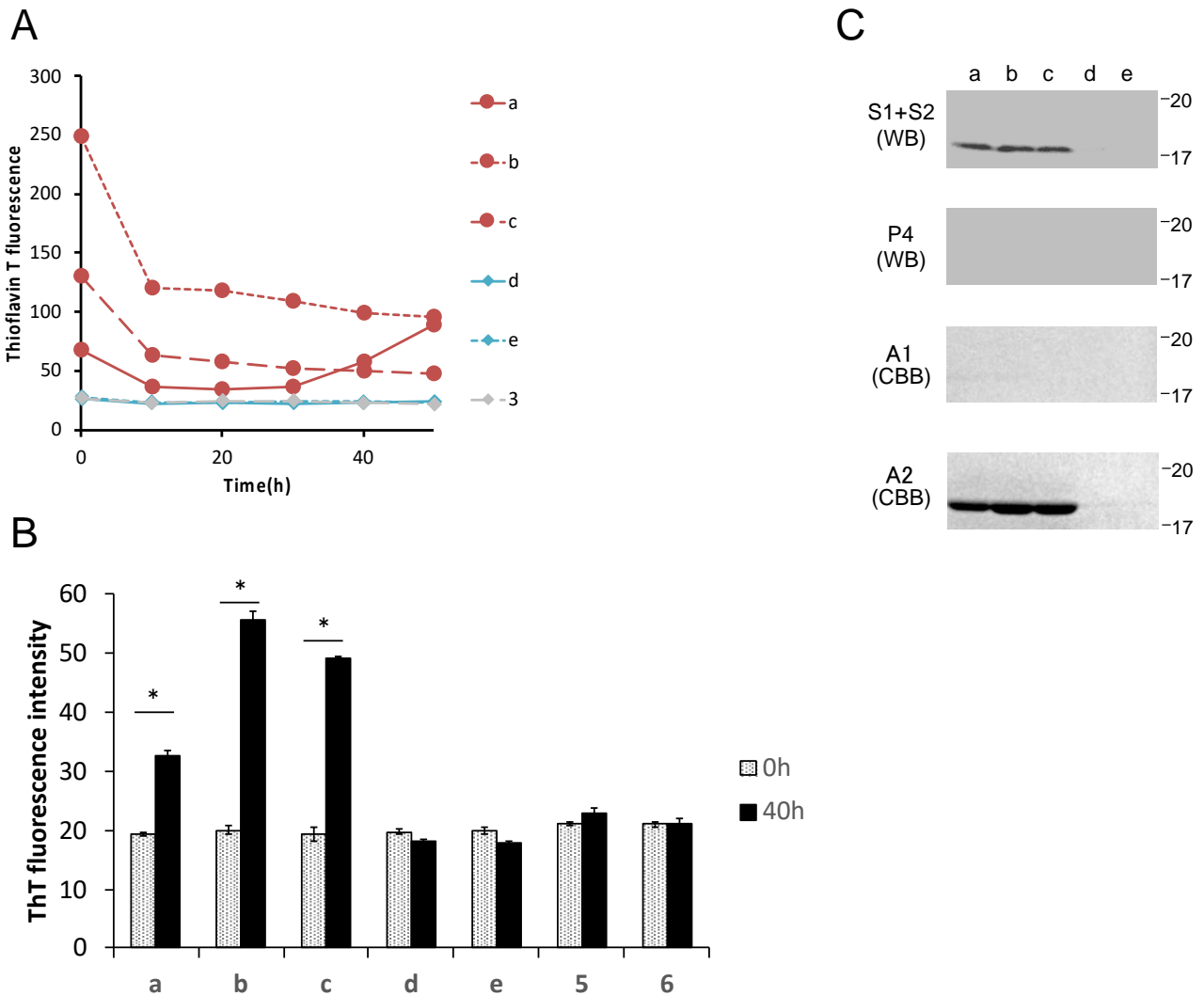A) The kinetics of recombinant mouse α-syn amyloid formation were monitored by ThT fluorescence. Recombinant mouse α-syn was incubated in solution A1 with 5% of the P4 fraction of mouse α-syn-injected mouse brain (circle). As control, the P4 fraction of PBS-injected mouse brain and only monomer were used for the reactions (diamond). (B) ThT fluorescence intensity of α-syn fibrils amplified by PMCA at 0 h and 40 h. (C) Fractions of mouse brains and amplified products using them as seeds were analyzed by WB stained with anti-α-syn antibody [ab209420(Abcam)]and CBB. After the seeding reaction and PMCA (A2) using the P4 fraction as a seed, mouse α-syn aggregates were amplified to a detectable level with CBB staining. *p < 0.01

3.4 The preparation of seed-enriched fraction from the human brains.

The samples obtained from Brain Bank in Japan were from the insular gyrus of MSA

patients, DLB patients, and controls (Table 2). SDS-insoluble pellet (P4) fractions were obtained

from these human brain tissue samples (Figure 8B). To examine in which fraction of the human

brain the pathologic α-syn accumulated, the S1+S2, P3 and P4 fractions of human brain

homogenates were analyzed by WB. Solubilized monomeric p-syn in S1+S2 fractions was detected

in for 4 out of 5 cases of MSA, 2 out of 5 cases of DLB, and 2 out of 5 cases of controls. The P3

fraction, which corresponds to the sarkosyl–insoluble fraction, displayed enriched p-syn in 4 out of 5

cases of MSA and 4 out of 5 cases of DLB (Figure 12). As signals of phosphorylated α-syn could not

be detected in the WB of the P4 fraction, a filter trap assay (FTA) was performed for each fraction,

as well as immunostaining of the smears of the P4 fraction. In the FTA, very weak signal of

phosphorylated α-syn was detected in the P4 fractions of DLB-4 by anti-p-syn antibody #64 (Wako)

(Figure 13).
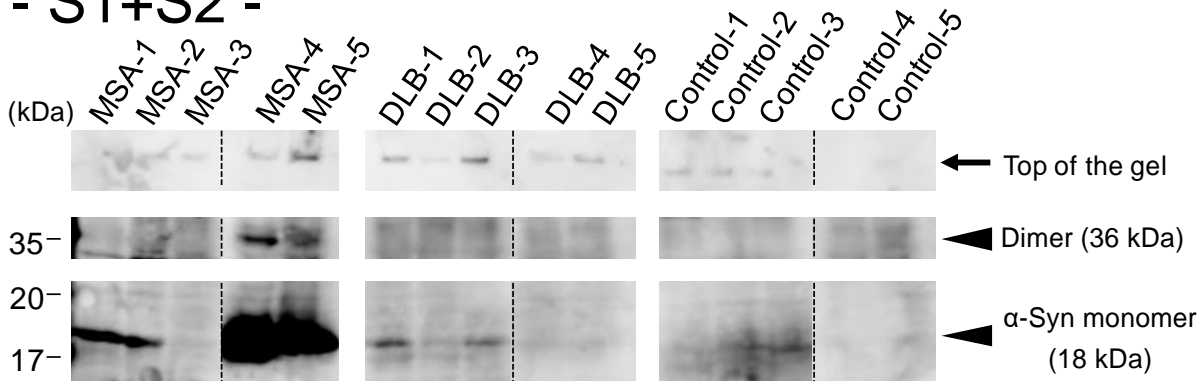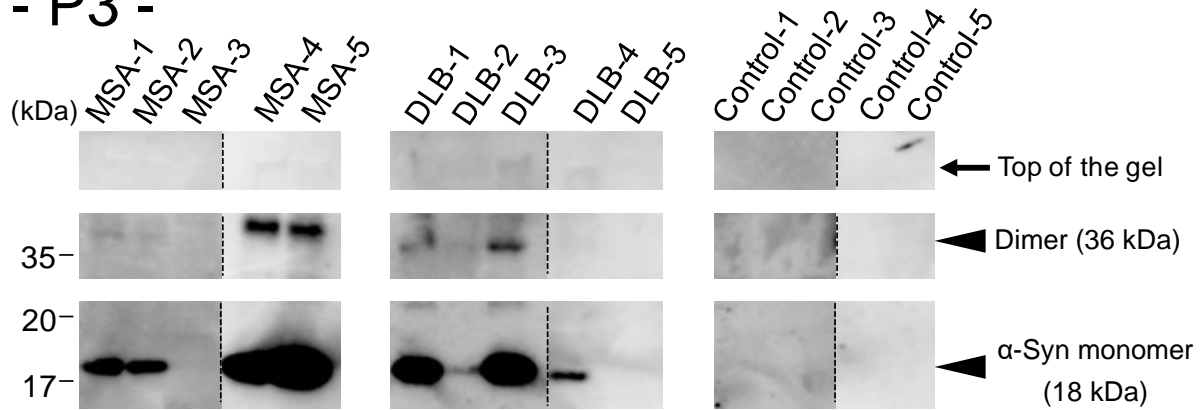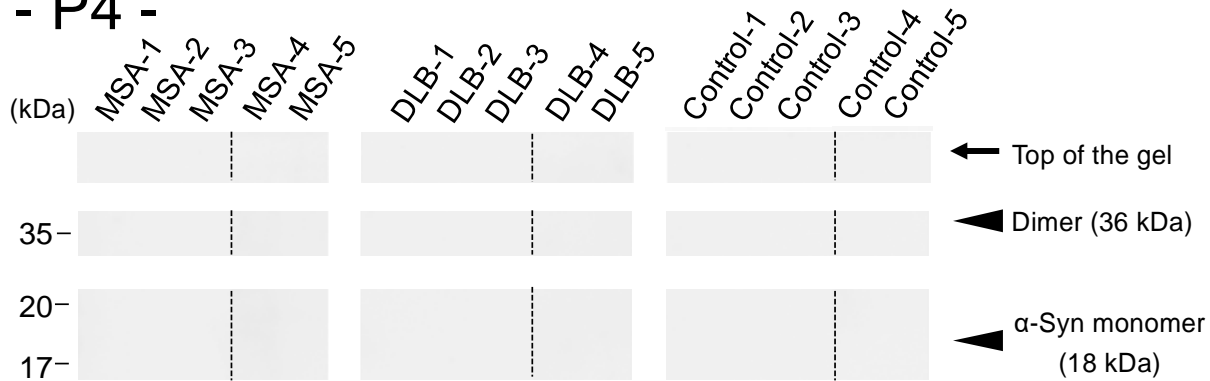
Figure 12. The S1+S2, P3 and P4 fractions were analyzed by Western blot (WB).

Signals of phosphorylated α-syn were detected in WB for the S1+S2 and the P3 fractions of α-synucleinopathy and some control brains, but they were not detected in WB of the P4 fraction. Anti-p-syn antibody #64 was used.
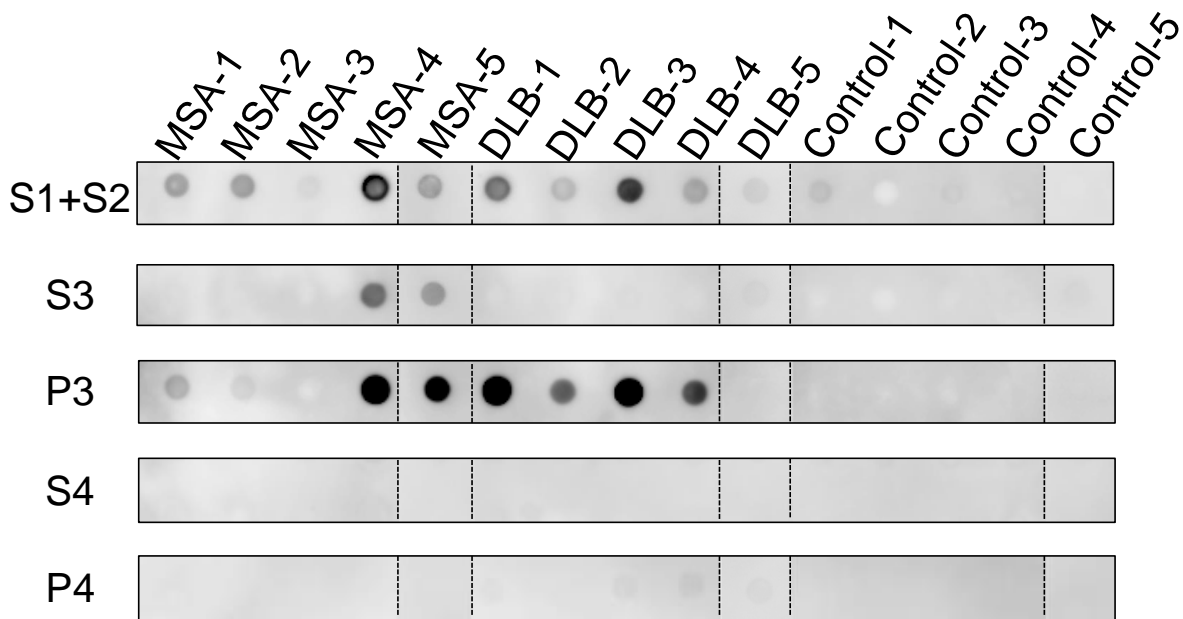
Figure 13. All fractions were analyzed by FTA

Signals of phosphorylated α-syn were detected in FTA of the P3 fractions of several diseased brains.

Furthermore, to detect the presence of disease-brain derived α-syn aggregates, immunochemical

analysis was performed on the smears of the P4 fraction with anti-p-syn antibody. Immunostaining

of the smears revealed p-syn immunoreactive materials in all of the diseased brains and in some of

the control brains (Control-2 and Control-3) (Figure 14). The amyloid seeding reactions of the P4

fractions from human brains were monitored with ThT (Figure 15). The ThT fluorescence intensity

of products after seeding reaction (A1), with the P4 fraction using human brains as seeds, revealed

42

an increase in 5 out of 5 MSA cases, 4 out of 5 DLB cases, and 3 out of 5 control cases. After the

seeding reaction and PMCA (A2), using the P4 fraction of the disease brains as seeds, a considerable

increase in the ThT fluorescence signal was observed compared to the control (Figure 16). The ThT

fluorescence intensity showed an increase in 5 out of 5 MSA cases, 5 out of 5 DLB cases, and 2 out

of 5 control cases. The amplified fractions by seeding reaction (A1) with the P4 fraction of the

diseased brains as a seed displayed α-syn immunoreactivity by WB stained with anti-α-syn antibody

[ab209420(Abcam)] in 5 out of 5 MSA cases, 5 out of 5 DLB cases, and 2 out of 5 control cases.

After PMCA amplification, CBB bands were detected in 5 out of 5 MSA cases, 5 out of 5 DLB,

cases and 1 out of 5 control cases (Figure 17). A sufficient amount of aggregates for proteinase

digestion experiments and MS analysis were obtained.
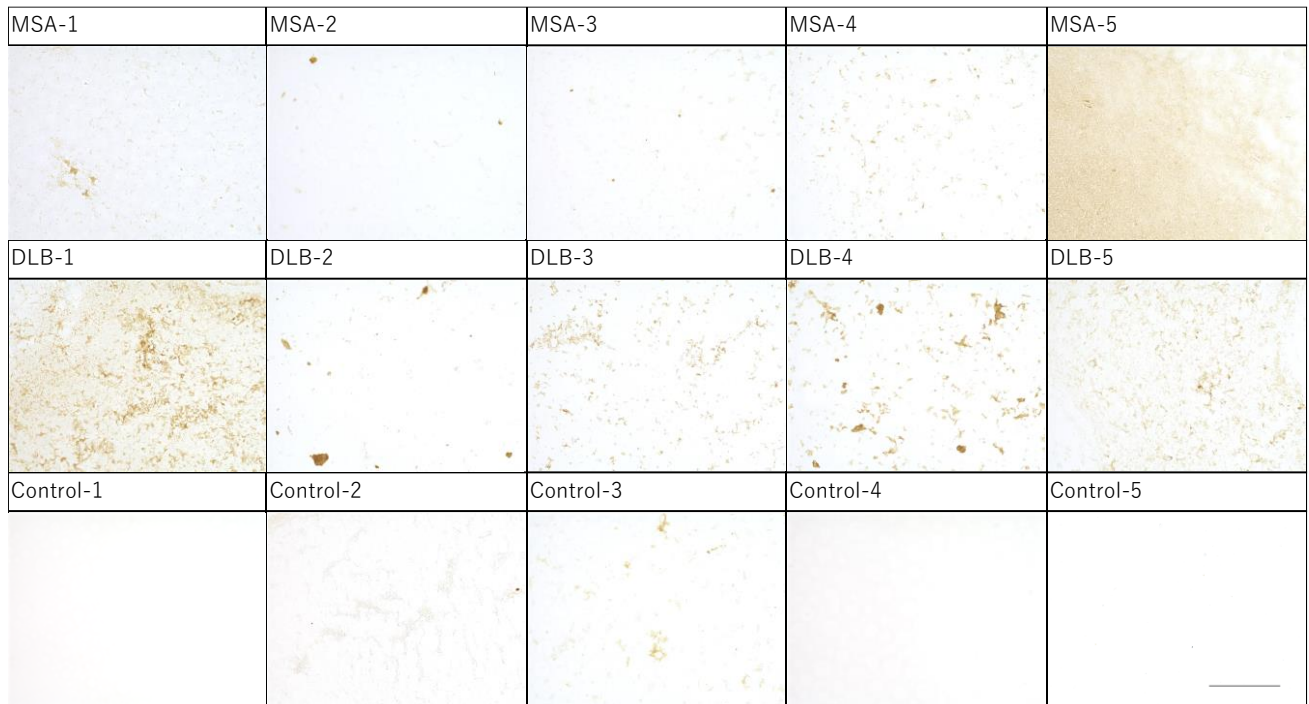
Figure 14. Immunostainings of the P4 fraction smears.

The P4 fractions of all of the diseased brains and a few of the control brains (Control-2 and Control-3) displayed positive signals with immunostaining with anti-p-syn antibody. Scale bar: 200 μm.
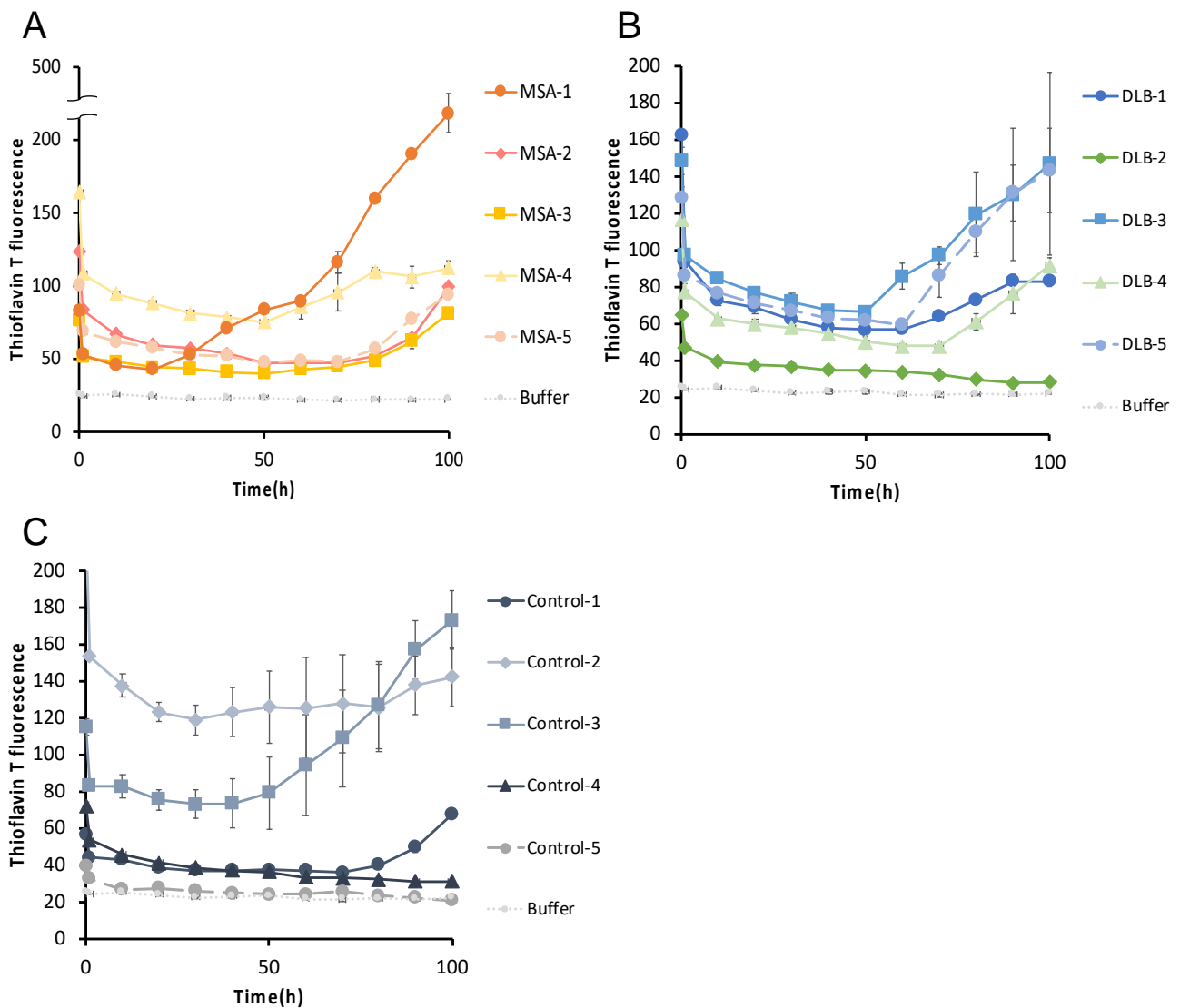
Figure 15. The seeding reactions of the P4 fractions of human brains.

The kinetics of recombinant human α-syn amyloid formation using the P4(A, B, C) fractions of human brains as seeds, monitored by ThT fluorescence. For the reaction control, no seeds buffer only were added. P4 fractions of diseased brains showed varying increases in fluorescence.
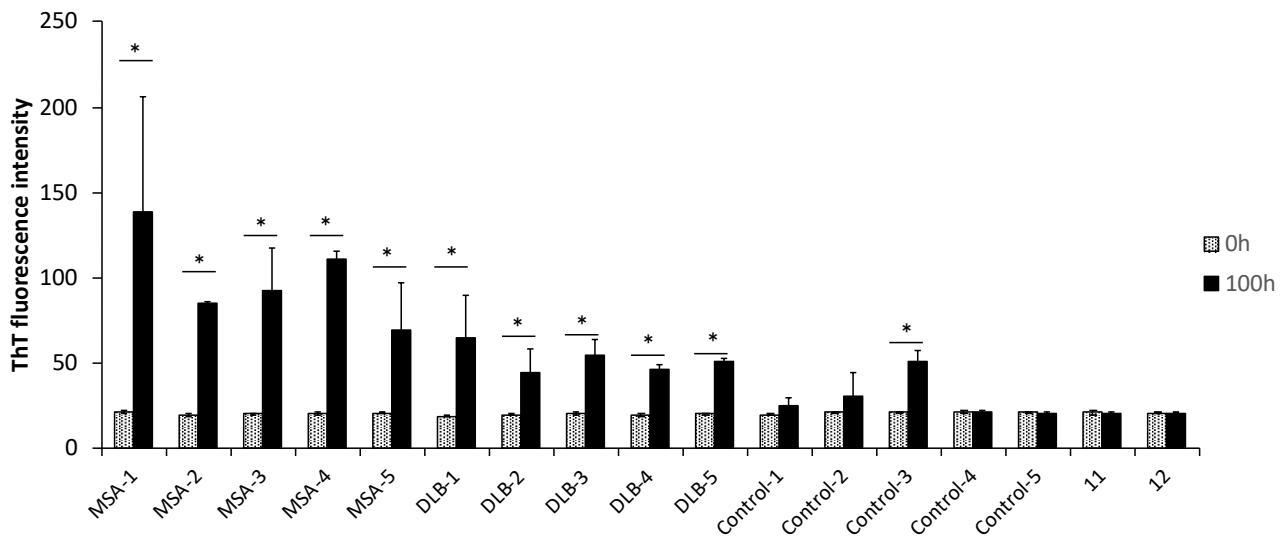
Figure 16. ThT fluoresc ence intensities of products after PMCA at 0 h and 100 h.

ThT fluorescence intensity of PMCA at 0 h and 100 h (10: Human PFF after seeding reaction; 11:

Buffer after seeding reaction; 12: Buffer). *p < 0.01
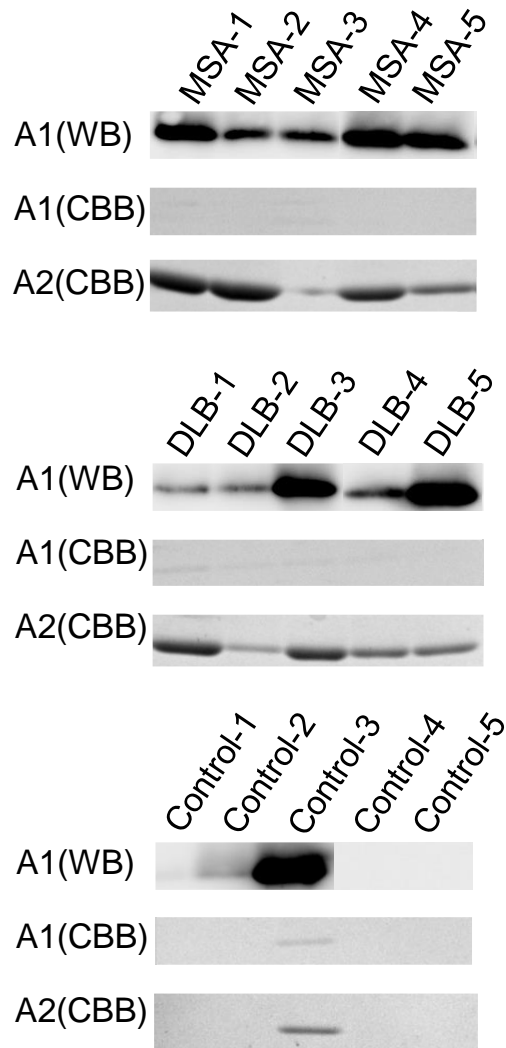
Figure 17. Amplified products using seeds derived from diseased and control brains were analyzed by WB and CBB.

WB was conducted with anti-α-syn antibody [ab209420(Abcam)]. After seeding reaction and PMCA (A2) using the P4 fraction as a seed, human α-syn aggregates were amplified to a detectable level via CBB staining.

3.5 The MALDI-TOF-MS analysis of proteinase K-resistant core

Spontaneously aggregated recombinant mouse and human α-syn were obtained and used as seeds. Amplified aggregates after seeding reaction (A1) and PMCA (A2) from recombinant α-syn were obtained. The properties of these aggregates were analyzed using proteinase digestion experiments. Proteinase K digestion-resistant cores of mouse and human α-syn aggregates after 120 min digestion were analyzed by MALDI-TOF-MS. The peaks were detected mostly at m/z 8.00×10^3, m/z 9.18×10^3, and m/z 1.11×10^4 for mouse α-syn PFFs and at m/z 8.00×10^3 and m/z 9.18×10^3, for aggregates after seeding reaction alone (A1) and for aggregates after both seeding reaction and PMCA (A2). The findings are similar to the previous findings of our group on the proteinase-resistant cores of mouse α-syn fibrils [22, 23]. The peaks were detected at m/z $6.36 - 6.38 \times 10^3$, m/z 1.09×10^4, m/z 1.13-1.14×10^4, and m/z 1.27-1.28×10^4 for human α-syn PFFs, aggregates after seeding reaction alone (A1) and after both seeding reaction and PMCA (A2). For A2, the peaks were also observed at m/z 7.32×10^3 and m/z 8.86×10^3. The results are also similar to those reported for the proteinase-resistant cores of human α-syn fibrils [23]. These findings indicate that the properties of PFFs are preserved after seeding reaction and PMCA.
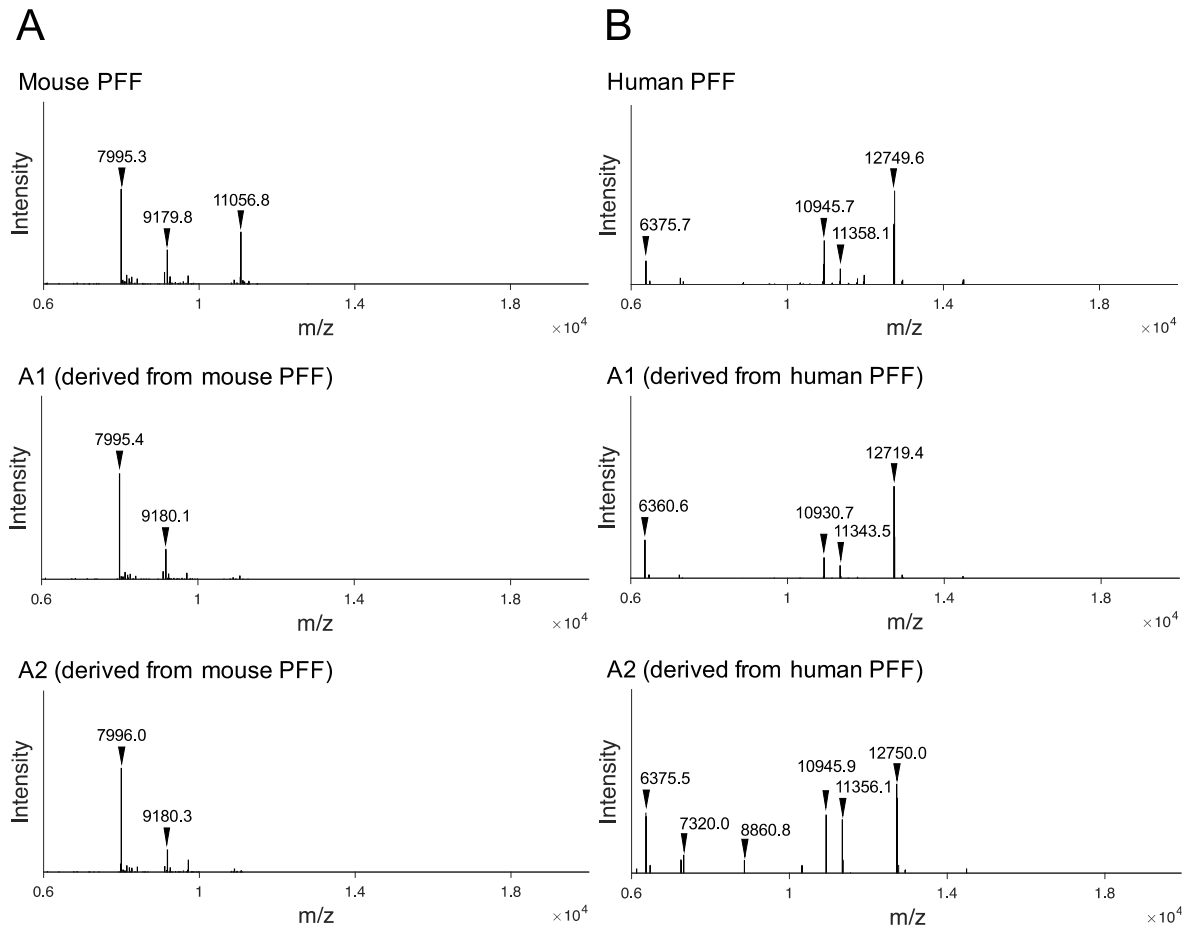
Figure 18. Preserved properties of recombinant mouse and human α-syn aggregates after seeding reaction and PMCA.

(A) MALDI-TOF MS spectra (m/z 6,000–20,000) of core peptides from mouse α-syn PFF and aggregates after only seeding reaction (A1) and both seeding reaction and PMCA (A2). The peaks for the proteinase-resistant fragment are indicated on the horizontal axis (m/z). (B) MALDI-TOF-MS spectra (m/z 6,000–20,000) of core peptides from human α-syn PFF and aggregates after only seeding reaction (A1) and both seeding reaction and PMCA (A2). The peaks for the proteinase-resistant fragment are indicated (m/z).

As a sufficient amount of aggregates for proteinase digestion experiments and MS analysis were obtained, proteinase digestion experiments were conducted to examine the differences in the biochemical properties of amplified α-syn aggregates from mouse brains and disease brains. Proteinase

K digestion-resistant cores were then examined with MALDI-TOF MS analysis. In mouse brains, the peaks were detected mostly at m/z 8.00 $\times10^3$, m/z 9.18 $\times10^3$, and m/z 1.11 $\times10^4$. The peaks are similar to those of the proteinase-resistant cores of mouse α-syn fibrils (Figure 19). In disease brains, the main peaks were detected at m/z 6.36 – 6.38 $\times10^3$, m/z 1.09 $\times10^4$, m/z 1.13-1.14 $\times10^4$, and m/z 1.27-1.28 $\times10^4$. The results are similar to that of human recombinant α-syn aggregates (Figure 20). No specific peaks for either MSA or DLB were observed. No data was obtained from MSA-3 due to technical errors. No data was obtained for normal brains, apart from Control-3, which exhibited p-syn signals in the P4 fraction and a CBB-positive α-syn band for A2.

A2 (derived from mouse α-syn injected mouse brain)_a

Intensity

7995.5

9180.0

0.6 ... 1 ... 1.4 ... 1.8

m/z ×10⁴

A2 (derived from mouse α-syn injected mouse brain)_b

Intensity

7995.7

9180.3

0.6 ... 1 ... 1.4 ... 1.8

m/z ×10⁴

A2 (derived from mouse α-syn injected mouse brain)_c

Intensity

7996.0

9180.6

0.6 ... 1 ... 1.4 ... 1.8

m/z ×10⁴
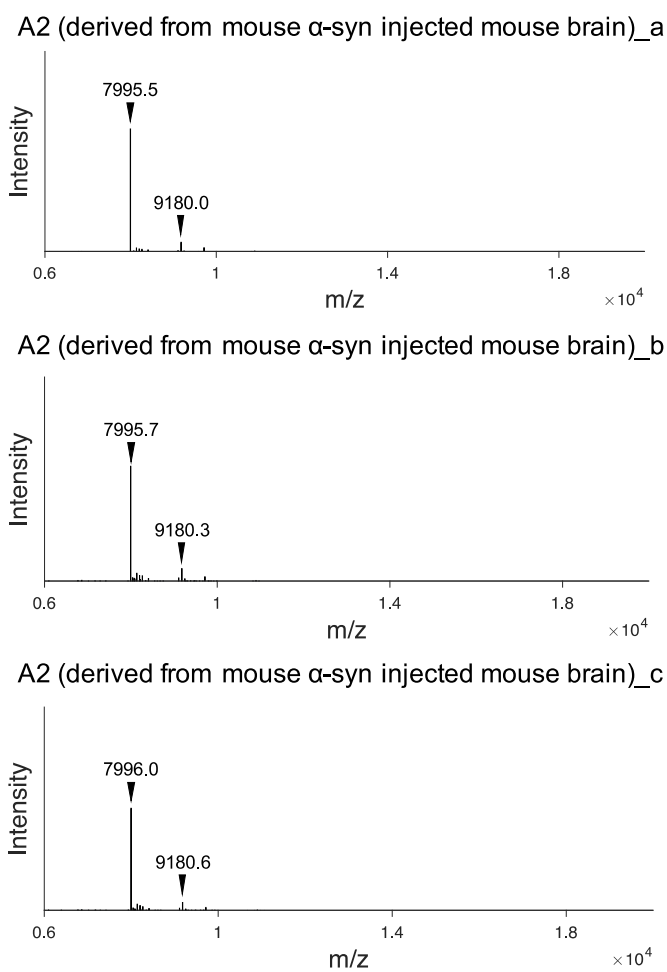
Figure 19. **MS analysis of the proteinase K-resistant cores of mouse brain aggregates.**

MALDI-TOF MS spectra (m/z 6,000–20,000) of proteinase K-resistant core peptides of A2. The same cores were detected among recombinant mouse α-syn aggregates and mouse brain aggregates.
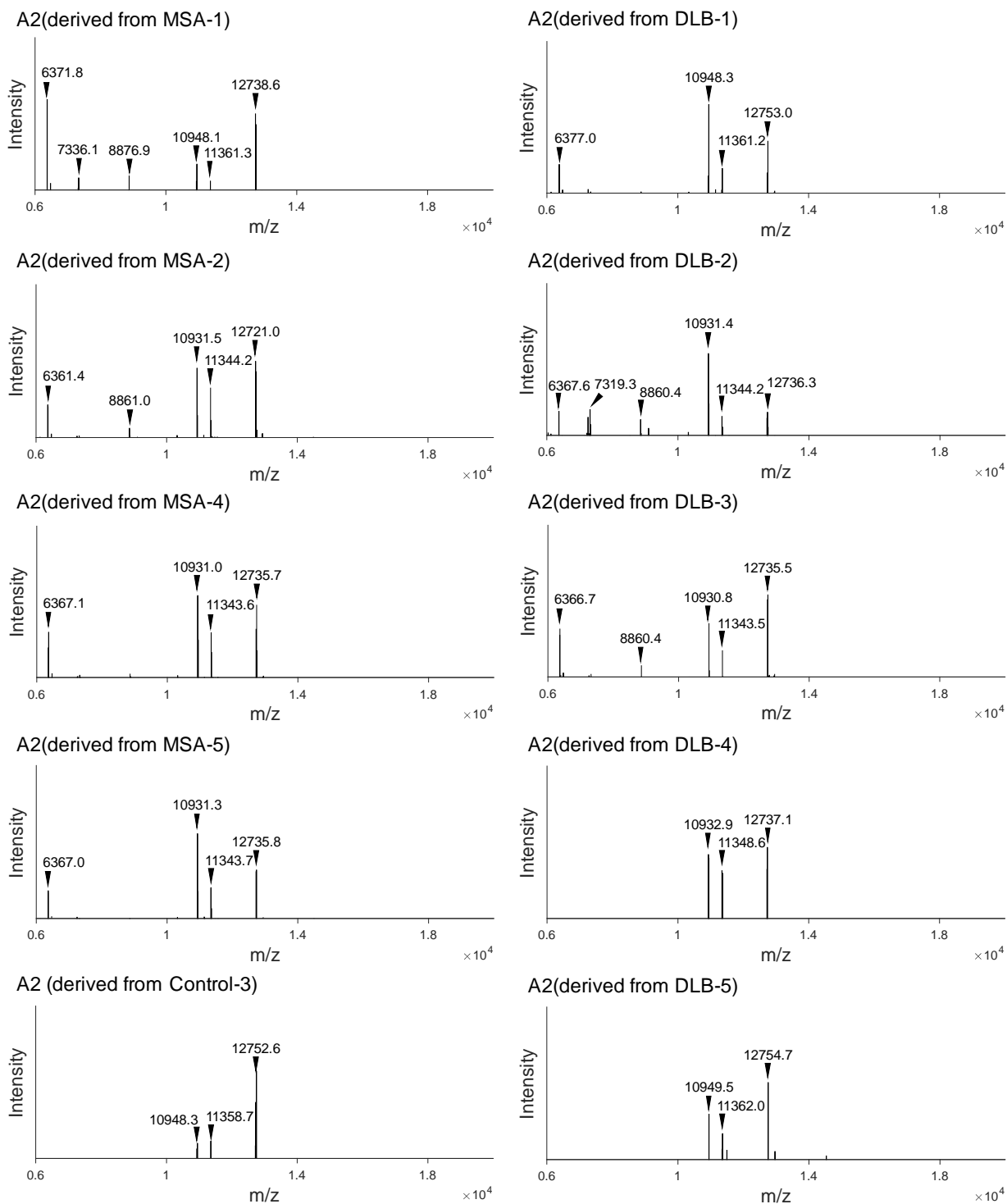
Figure 20. MS analysis of the proteinase K-resistant cores of MSA and DLB aggregates.

MALDI-TOF MS spectra (m/z 6,000–20,000) of proteinase K-resistant core peptides of A2. No obvious difference between cases was observed.

52

3.6 Electron microscopy

To identify the structural differences between synucleinopathies, EM was used to observe A2 between MSA and DLB brains. No obvious structural differences between fibrils of A2 derived from MSA and DLB brains were observed. No fibrils as a result of A2 were detected from Control-1, Control-4, and Control-5, as well as MSA-5 and DLB-2. However, for MSA-5 and DLB-2, it is suspected that the reason no fibrils were detected is due to technical errors.
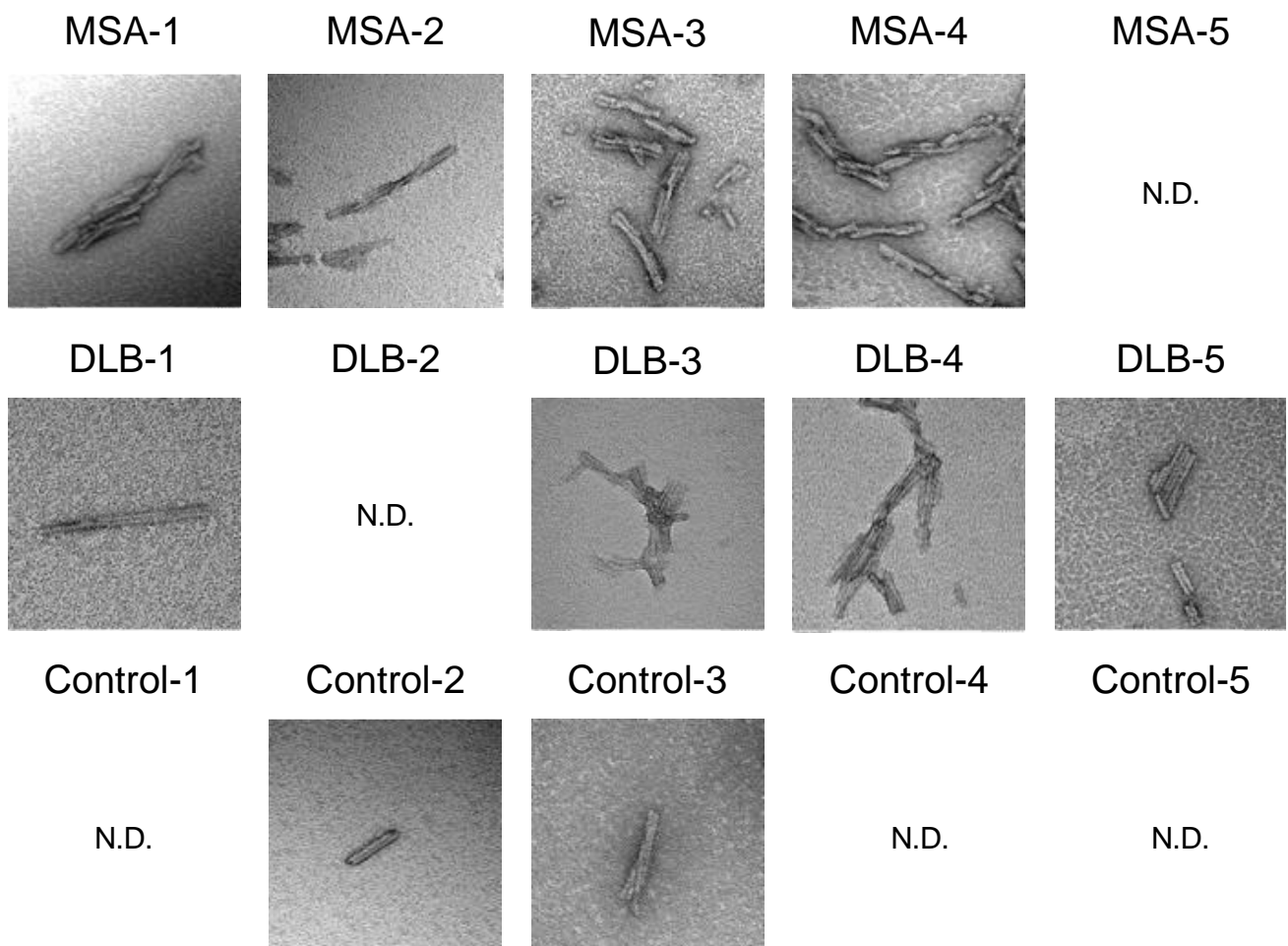
Figure 21. Electron microscopy of amplified α-syn derived from synucleinopathies

Electron microscopy of A2. In those fibrils from MSA-5, DLB-2, Control-1, Control-4 and Control-5 were not detectable.

Chapter 4. Discussion

In this thesis, our established method enabled the amplification and analysis of very low amounts of α-syn from synucleinopathies. PMCA made it possible to detect very low concentrations of misfolded human α-syn. In addition, the α-syn fibril core was shown to be preserved based on the results of MS analysis of the proteinase K-resistant core of the α-syn pre and post not only seeding reaction but also PMCA. Phosphorylated α-syn aggregates were detected in SDS-insoluble pellets from DLB and MSA brains by immunostaining. The combination method of seeding reaction and PMCA allowed for the amplification of α-syn aggregates of synucleinopathies more than ever reported previously.

4.1 PMCA of misfolded α-syn

In previous studies, the reaction efficiency of PMCA of misfolded α-syn was investigated by computational chemistry, and the possibility to detect up to 2 pg was suggested [37]. However, no previous reports have experimentally detected down to this level. PMCA of misfolded prions in diseased brains allows detection of femto-level concentrations because self-aggregation occurs minimally [46]. In this paper, misfolded α-syn from femto-level could be detected. In addition, by carefully choosing the conditions to avoid the effects of self-aggregation, abnormal α-syn from at least 50 fM used as a seed was detected, which is a smaller amount of misfolded α-syn detected compared to previous studies.

4.2 The necessity to amplify misfolded α-syn

α-syn is a major component of cytoplasmic inclusions, such as Lewy bodies in PD and DLB and glial cytoplasmic inclusions in MSA [12, 47]. Several recent studies have presented evidence for the existence of conformational strains for misfolded aggregates made of α-syn [25, 48]. These studies used either recombinant α-syn aggregates or self-propagated α-syn aggregates induced by either recombinant α-syn seeds or Sarkosyl-insoluble proteins in the mouse brains. Our group also recently

has reported MS analysis and electron microscopic analysis showing the sequence- and seed-structure-dependent polymorphism of α-syn fibrils [22, 23]. To apply these methods to α-synucleinopathies, a sufficient amount of α-syn aggregates was required for MS analysis.

PMCA was used to amplify α-syn aggregates from the seed. α-syn aggregates that formed spontaneously *in vitro* from recombinant α-syn and those formed by seeding reaction and PMCA using recombinant α-syn aggregates as seeds were obtained. After amplification, sufficient amounts of α-syn aggregates were obtained, enough to be detected in SDS-PAGE with CBB staining. As a result, with those aggregates, proteinase K-resistant cores were detected in distinct ways between human and mouse α-syn aggregates by MS analysis. These cores were preserved after the seeding reaction and PMCA. As the core structure of the seeds was preserved, analysis of the resulting amplified α-syn could be done without worry of structural differences present.

4.3 The detection of phosphorylated α-syn

Amplified α-syn aggregates were obtained using seeds derived from MSA and DLB brains. The fraction which was enriched with α-syn aggregates was examined. For WB, the enhanced method via combined fixation with 4% PFA and 0.01% glutaraldehyde was used [42]. This fixation produced

an approximately 10-fold increase in sensitivity that enabled us to detect both total and Ser129-phosphorylated α-syn even at a concentration of approximately 250 pg of total α-syn. The phosphorylated α-syn of P4 was not detected in the WB and FTA, but it could be detected by immunostaining. Thus, α-syn in the P4 fractions were suspected to be less than 250 pg. Phosphorylated α-syn aggregates in P4 fractions were detected by immunostaining that allowed detection of each visible aggregate.

4.4 The proteinase-K resistant cores by MS analysis

As it is suspected that difference in structure leads to different disease phenotypes, core structures in amplified samples from MSA and DLB were analyzed. MSA and DLB have distinct pathologies despite being both caused by α-syn.

This P4 fraction was used as a seed to amplify α-syn aggregates, and, after seeding reaction and PMCA, CBB detectable α-syn was obtained in the cases exhibiting the immunoreactivity of p-syn in the smears of P4.

After 120 min of proteinase K treatment, MS analyses of those proteinase K-resistant cores were conducted. The findings revealed same peaks as those of the proteinase K-resistant cores of

recombinant human α-syn aggregates (Figure 18 and Figure 20). There were no significant differences between the peaks of MSA and DLB.

This finding indicates either that α-syn aggregates of MSA and DLB have identical structures or that our methods determining the proteinase-K resistant cores by MS are not adequately sensitive to distinguish those structures.

4.5 The structural differences between synucleinopathies by EM

To identify the structural differences between synucleinopathies, EM was used to observe amplified human α-syn derived from MSA and DLB brains. Several studies have presented evidence for the existence of conformational strains for misfolded aggregates made up of α-syn [5]. Amplified human α-syn from MSA brains are more likely to form twisted types of fibrils. Conversely, amplified human α-syn from DLB are more likely to form ribbon types of fibrils [4, *in vivo*]. However, the long α-syn fibrils could not be observed in this paper(Figure 21). This result may be because the excessive sonication after PMCA, which reduces the lengths of α-syn fibrils from each synucleinopathy, not adequate to differentiate the structural features.

4.6 α-syn of control brain samples

P-syn immunoreactivity in P4 of control-2 and control-3 were detected as well as in the WB of the S1+S2 brain homogenates. These controls exhibited no clinical symptoms of synucleinopathy as well as no LB score (*Table 1*). It is possible that these control brains have presymptomatic synucleinopathies. Recent studies have amplified the cerebrospinal fluid of DLB and PD patients using RT-QuIC, detecting misfolded α-syn [49]. In a similar manner, the combined seeding reaction and PMCA may be able to detect misfolded α-syn also in presymptomatic brains. Further survey of the existence of p-syn immunoreactivity in P4 fraction of control brains is important.

4.7 Further study and recommendation

Further studies using other methods, such as electron microscope or MS analysis of partial digestion by proteinase are needed. However, these analyses on the amplified abnormal proteins from disease brains could be used to study other neurodegenerative disorders.

References

[1] T.J. Paul, J. Hardy, K.H. Fischbeck, Toxic Proteins in Neurodegenerative Disease, Science (2002).

[2] C.A. Ross, M.A. Poirier, Protein aggregation and neurodegenerative disease, Nat Med 10 Suppl (2004) S10-17. 10.1038/nm1066.

[3] M. Jucker, L.C. Walker, Self-propagation of pathogenic protein aggregates in neurodegenerative diseases, Nature 501 (2013) 45-51. 10.1038/nature12481.

[4] C. Soto, Unfolding the role of protein misfolding in neurodegenerative diseases, Nat Rev Neurosci 4 (2003) 49-60. 10.1038/nrn1007.

[5] C. Soto, S. Pritzkow, Protein misfolding, aggregation, and conformational strains in neurodegenerative diseases, Nat Neurosci 21 (2018) 1332-1340. 10.1038/s41593-018-0235-9.

[6] A.W. Fitzpatrick, G.T. Debelouchina, M.J. Bayro, D.K. Clare, M.A. Caporini, V.S. Bajaj, C.P. Jaroniec, L. Wang, V. Ladizhansky, S.A. Muller, C.E. MacPhee, C.A. Waudby, H.R. Mott, A. De Simone, T.P. Knowles, H.R. Saibil, M. Vendruscolo, E.V. Orlova, R.G. Griffin, C.M. Dobson, Atomic structure and hierarchical assembly of a cross-beta amyloid fibril, Proc Natl Acad Sci U S A 110 (2013) 5468-5473. 10.1073/pnas.1219476110.

[7] L. Giehm, N. Lorenzen, D.E. Otzen, Assays for alpha-synuclein aggregation, Methods 53 (2011) 295-305. 10.1016/j.ymeth.2010.12.008.

[8] F.N. Emamzadeh, Alpha-synuclein structure, functions, and interactions, J Res Med Sci 21 (2016) 29. 10.4103/1735-1995.181989.

[9] T.S. Ulmer, A. Bax, N.B. Cole, R.L. Nussbaum, Structure and dynamics of micelle-bound human alpha-synuclein, J Biol Chem 280 (2005) 9595-9603. 10.1074/jbc.M411805200.

[10] C.C. Jao, B.G. Hegde, J. Chen, I.S. Haworth, R. Langen, Structure of membrane-bound alpha-synuclein from site-directed spin labeling and computational refinement, Proc Natl Acad Sci U S A 105 (2008) 19666-19671. 10.1073/pnas.0807826105.

[11] C.R. Bodner, C.M. Dobson, A. Bax, Multiple tight phospholipid-binding modes of alpha-synuclein revealed by solution NMR spectroscopy, J Mol Biol 390 (2009) 775-790. 10.1016/j.jmb.2009.05.066.

[12] M.G. Spillantini, R.A. Crowther, R. Jakes, N.J. Cairns, P.L. Lantos, M. Goedert, Filamentous alpha-synuclein inclusions link multiple system atrophy with Parkinson's disease and dementia with Lewy bodies, Neurosci Lett 251 (1998) 205-208. 10.1016/s0304-3940(98)00504-7.

[13] C. Wang, C. Zhao, D. Li, Z. Tian, Y. Lai, J. Diao, C. Liu, Versatile Structures of alpha-Synuclein, Front Mol Neurosci 9 (2016) 48. 10.3389/fnmol.2016.00048.

[14] H. Fujiwara, M. Hasegawa, N. Dohmae, A. Kawashima, E. Masliah, M.S. Goldberg, J. Shen, K. Takio, T. Iwatsubo, alpha-Synuclein is phosphorylated in synucleinopathy lesions, Nat Cell Biol 4 (2002) 160-164. 10.1038/ncb748.

[15] J.P. Anderson, D.E. Walker, J.M. Goldstein, R. de Laat, K. Banducci, R.J. Caccavello, R. Barbour, J. Huang, K. Kling, M. Lee, L. Diep, P.S. Keim, X. Shen, T. Chataway, M.G. Schlossmacher, P. Seubert, D. Schenk, S. Sinha, W.P. Gai, T.J. Chilcote, Phosphorylation of Ser-129 is the dominant pathological modification of alpha-synuclein in familial and sporadic Lewy body disease, J Biol Chem 281 (2006) 29739-29752. 10.1074/jbc.M600933200.

[16] H. McCann, C.H. Stevens, H. Cartwright, G.M. Halliday, α-Synucleinopathy phenotypes, Parkinsonism & Related Disorders 20 (2014) S62-S67. 10.1016/s1353-8020(13)70017-8.

[17] H.M. Gao, P.T. Kotzbauer, K. Uryu, S. Leight, J.Q. Trojanowski, V.M. Lee, Neuroinflammation and oxidation/nitration of alpha-synuclein linked to dopaminergic neurodegeneration, J Neurosci 28 (2008) 7687-7698. 10.1523/jneurosci.0143-07.2008.

[18] Y.E. Kim, M.S. Hipp, A. Bracher, M. Hayer-Hartl, F.U. Hartl, Molecular chaperone functions in protein folding and proteostasis, Annu Rev Biochem 82 (2013) 323-355. 10.1146/annurev-biochem-060208-092442.

[19] D.J. Irwin, V.M. Lee, J.Q. Trojanowski, Parkinson's disease dementia: convergence of alpha-synuclein, tau and amyloid-beta pathologies, Nat Rev Neurosci 14 (2013) 626-636. 10.1038/nrn3549.

[20] A.L. Woerman, The importance of developing strain-specific models of neurodegenerative disease, Acta Neuropathol 134 (2017) 809-812. 10.1007/s00401-017-1761-3.

[21] M.H. Polymeropoulos, C. Lavedan, E. Leroy, S.E. Ide, A. Dehejia, A. Dutra, B. Pike, H. Root, J. Rubenstein, R. Boyer, E.S. Stenroos, S. Chandrasekharappa, A. Athanassiadou, T. Papapetropoulos, W.G. Johnson, A.M. Lazzarini, R.C. Duvoisin, G. Di Iorio, L.I. Golbe, R.L. Nussbaum, Mutation in the alpha-synuclein gene identified in families with Parkinson's disease, Science 276 (1997) 2045-2047. 10.1126/science.276.5321.2045.

[22] G. Tanaka, T. Yamanaka, Y. Furukawa, N. Kajimura, K. Mitsuoka, N. Nukina, Biochemical and morphological classification of disease-associated alpha-synuclein mutants aggregates, Biochem Biophys Res Commun 508 (2019) 729-734. 10.1016/j.bbrc.2018.11.200.

[23] G. Tanaka, T. Yamanaka, Y. Furukawa, N. Kajimura, K. Mitsuoka, N. Nukina, Sequence- and seed-structure-dependent polymorphic fibrils of alpha-synuclein, Biochim Biophys Acta Mol Basis Dis 1865 (2019) 1410-1420. 10.1016/j.bbadis.2019.02.013.

[24] D.W. Sanders, S.K. Kaufman, S.L. DeVos, A.M. Sharma, H. Mirbaha, A. Li, S.J. Barker, A.C. Foley, J.R. Thorpe, L.C. Serpell, T.M. Miller, L.T. Grinberg, W.W. Seeley, M.I. Diamond, Distinct tau prion strains propagate in cells and mice and define different tauopathies, Neuron 82 (2014) 1271-1288. 10.1016/j.neuron.2014.04.047.

[25] W. Peelaerts, L. Bousset, A. Van der Perren, A. Moskalyuk, R. Pulizzi, M. Giugliano, C. Van den Haute, R. Melki, V. Baekelandt, alpha-Synuclein strains cause distinct synucleinopathies after local and systemic administration, Nature 522 (2015) 340-344. 10.1038/nature14547.

[26] B. Li, P. Ge, K.A. Murray, P. Sheth, M. Zhang, G. Nair, M.R. Sawaya, W.S. Shin, D.R. Boyer, S. Ye, D.S. Eisenberg, Z.H. Zhou, L. Jiang, Cryo-EM of full-length alpha-synuclein reveals fibril polymorphs with a common structural kernel, Nat Commun 9 (2018) 3609. 10.1038/s41467-018-05971-2.

[27] N.A. Mabbott, How do PrP(Sc) Prions Spread between Host Species, and within Hosts?, Pathogens 6 (2017). 10.3390/pathogens6040060.

[28] S.B. Prusiner, Prions, Proc Natl Acad Sci U S A 95 (1998) 13363-13383. 10.1073/pnas.95.23.13363.

[29] I. Moreno-Gonzalez, C. Soto, Misfolded protein aggregates: mechanisms, structures and potential for disease transmission, Semin Cell Dev Biol 22 (2011) 482-487. 10.1016/j.semcdb.2011.04.002.

[30] J.A. Johnston, C.L. Ward, R.R. Kopito, Aggresomes: a cellular response to misfolded proteins, J Cell Biol 143 (1998) 1883-1898. 10.1083/jcb.143.7.1883.

[31] K. Gousset, E. Schiff, C. Langevin, Z. Marijanovic, A. Caputo, D.T. Browman, N. Chenouard, F. de Chaumont, A. Martino, J. Enninga, J.C. Olivo-Marin, D. Mannel, C. Zurzolo, Prions hijack tunnelling nanotubes for intercellular spread, Nat Cell Biol 11 (2009) 328-336. 10.1038/ncb1841.

[32] J. Castilla, P. Saa, C. Soto, Detection of prions in blood, Nat Med 11 (2005) 982-985. 10.1038/nm1286.

[33] R.C. Angers, S.R. Browning, T.S. Seward, C.J. Sigurdson, M.W. Miller, E.A. Hoover, G.C. Telling, Prions in skeletal muscles of deer with chronic wasting disease, Science 311 (2006) 1117. 10.1126/science.1122864.

[34] J.D. Harper, P.T. Lansbury, Jr., Models of amyloid seeding in Alzheimer's disease and scrapie: mechanistic truths and physiological consequences of the time-dependent solubility of amyloid proteins, Annu Rev Biochem 66 (1997) 385-407. 10.1146/annurev.biochem.66.1.385.

[35] G.P. Saborio, B. Permanne, C. Soto, Sensitive detection of pathological prion protein by cyclic amplification of protein misfolding, Nature 411 (2001) 810-813. 10.1038/35081095.

[36] V. Meyer, P.D. Dinkel, E. Rickman Hager, M. Margittai, Amplification of Tau fibrils from minute quantities of seeds, Biochemistry 53 (2014) 5804-5809. 10.1021/bi501050g.

[37] S. Paciotti, G. Bellomo, L. Gatticchi, L. Parnetti, Are We Ready for Detecting alpha-Synuclein Prone to Aggregation in Patients? The Case of "Protein-Misfolding Cyclic Amplification" and "Real-Time Quaking-Induced Conversion" as Diagnostic Tools, Front Neurol 9 (2018) 415. 10.3389/fneur.2018.00415.

[38] A. Okuzumi, M. Kurosawa, T. Hatano, M. Takanashi, S. Nojiri, T. Fukuhara, T. Yamanaka, H. Miyazaki, S. Yoshinaga, Y. Furukawa, T. Shimogori, N. Hattori, N. Nukina, Rapid dissemination of alpha-synuclein seeds through neural circuits in an in-vivo prion-like seeding experiment, Acta Neuropathol Commun 6 (2018) 96. 10.1186/s40478-018-0587-0.

[39] J.L. Whitwell, S.D. Weigand, M.M. Shiung, B.F. Boeve, T.J. Ferman, G.E. Smith, D.S. Knopman, R.C. Petersen, E.E. Benarroch, K.A. Josephs, C.R. Jack, Jr., Focal atrophy in dementia with Lewy bodies on MRI: a distinct pattern from Alzheimer's disease, Brain 130 (2007) 708-719. 10.1093/brain/awl388.

[40] O.A. Morozova, Z.M. March, A.S. Robinson, D.W. Colby, Conformational features of tau fibrils from Alzheimer's disease brain are faithfully propagated by unmodified recombinant protein, Biochemistry 52 (2013) 6960-6967. 10.1021/bi400866w.

[41] M. Masuda-Suzukake, T. Nonaka, M. Hosokawa, T. Oikawa, T. Arai, H. Akiyama, D.M. Mann, M. Hasegawa, Prion-like spreading of pathological alpha-synuclein in brain, Brain 136 (2013) 1128-1138. 10.1093/brain/awt037.

[42] A. Sasaki, S. Arawaka, H. Sato, T. Kato, Sensitive western blotting for detection of endogenous Ser129-phosphorylated alpha-synuclein in intracellular and extracellular spaces, Sci Rep 5 (2015) 14211. 10.1038/srep14211.

[43] P.O. Bauer, H.K. Wong, F. Oyama, A. Goswami, M. Okuno, Y. Kino, H. Miyazaki, N. Nukina, Inhibition of Rho kinases enhances the degradation of mutant huntingtin, J Biol Chem 284 (2009) 13153-13164. 10.1074/jbc.M809229200.

[44] Y. Saito, A. Kawashima, N.N. Ruberu, H. Fujiwara, S. Koyama, M. Sawabe, T. Arai, H. Nagura, H. Yamanouchi, M. Hasegawa, T. Iwatsubo, S. Murayama, Accumulation of phosphorylated alpha-synuclein in aging human brain, J Neuropathol Exp Neurol 62 (2003) 644-654. 10.1093/jnen/62.6.644.

[45] M. Hasegawa, H. Fujiwara, T. Nonaka, K. Wakabayashi, H. Takahashi, V.M. Lee, J.Q. Trojanowski, D. Mann, T. Iwatsubo, Phosphorylated alpha-synuclein is ubiquitinated in alpha-synucleinopathy lesions, J Biol Chem 277 (2002) 49071-49076. 10.1074/jbc.M208046200.

[46] C.J. Johnson, J.M. Aiken, D. McKenzie, M.D. Samuel, J.A. Pedersen, Highly efficient amplification of chronic wasting disease agent by protein misfolding cyclic amplification with beads (PMCAb), PLoS One 7 (2012) e35383. 10.1371/journal.pone.0035383.

[47] M. Baba, S. Nakajo, P.H. Tu, T. Tomita, K. Nakaya, V.M. Lee, J.Q. Trojanowski, T. Iwatsubo, Aggregation of alpha-synuclein in Lewy bodies of sporadic Parkinson's disease and dementia with Lewy bodies, Am J Pathol 152 (1998) 879-884.

[48] J.L. Guo, D.J. Covell, J.P. Daniels, M. Iba, A. Stieber, B. Zhang, D.M. Riddle, L.K. Kwong, Y. Xu, J.Q. Trojanowski, V.M. Lee, Distinct alpha-synuclein strains differentially promote tau inclusions in neurons, Cell 154 (2013) 103-117. 10.1016/j.celgaol.2013.05.057.

[49] G. Fairfoul, L.I. McGuire, S. Pal, J.W. Ironside, J. Neumann, S. Christie, C. Joachim, M. Esiri, S.G. Evetts, M. Rolinski, F. Baig, C. Ruffmann, R. Wade-Martins, M.T. Hu, L. Parkkinen, A.J. Green, Alpha-synuclein RT-QuIC in the CSF of patients with alpha-synucleinopathies, Ann Clin Transl Neurol 3 (2016) 812-818. 10.1002/acn3.338.